

Synthesis and Electronic Structure Studies of a Cr-Imido Redox Series

Supporting Information

Yuyang Dong, Ryan M. Clarke, Shao-Liang Zheng and Theodore A. Betley

Department of Chemistry and Chemical Biology

Harvard University

12 Oxford Street, Cambridge, MA 02138

General Considerations	3
Characterization and Physical Measurements	3
Metal Complexes Synthesis	4
Figure S1. UV-Vis Spectrum of $[(^{\text{AdF}}\text{L})\text{CrCl}]_2$ (2) and $(^{\text{AdF}}\text{L})\text{Cr}(\text{OTf})(\text{THF})_2$ (3)	9
Figure S2. Cyclic voltammogram of $[(^{\text{AdF}}\text{L})\text{CrCl}]_2$ (2)	10
Figure S3. Frozen 2-methyl tetrahydrofuran EPR spectrum of transiently stable chromium (I) species 4 at 77 K	11
Figure S4a. Full filed frozen toluene EPR spectrum of $(^{\text{AdF}}\text{L})\text{Cr}(\text{NMes})_2$ (5) at 77 K.....	12
Figure S4b. Zoomed-in frozen toluene EPR spectrum of $(^{\text{AdF}}\text{L})\text{Cr}(\text{NMes})_2$ (5) at 77 K.	13
Figure S5a. Frozen toluene EPR spectrum of $(^{\text{AdF}}\text{L})\text{Cr}(\text{NMes})(\text{THF})$ (8) at 77 K.....	14
Figure S5b. Zoomed-in frozen toluene EPR spectrum of $(^{\text{AdF}}\text{L})\text{Cr}(\text{NMes})(\text{THF})$ (8) at 77 K....	15
Figure S6. Frontier molecular orbital diagram showing metal d-orbitals for 6	16
Figure S7. Frontier molecular orbital diagram showing metal d-orbitals for 7	17
Figure S8. Frontier molecular orbital diagram showing metal d-orbitals for 8	18
Table S1. Bond Metrics Comparison Between DFT Optimized and Solid-State Molecular Structures	19
X-Ray Diffraction Techniques	20
Table S2. X-ray diffraction experimental details.....	22
Figure S9. Solid-state molecular structure for $[(^{\text{AdF}}\text{L})\text{CrCl}]_2$ (2).....	24
Figure S10. Solid-state molecular structure for $(^{\text{AdF}}\text{L})\text{Cr}(\text{OTf})(\text{THF})_2$ (3).....	25
Figure S11. Solid-state molecular structure for $(^{\text{AdF}}\text{L})\text{Cr}(\text{NMes})_2$ (5).....	26
Figure S12. Solid-state molecular structure for $(^{\text{AdF}}\text{L})\text{Cr}(\text{NMes})\text{Cl}$ (6)	27
Figure S13. Solid-state molecular structure for $(^{\text{AdF}}\text{L})\text{Cr}(\text{NMes})(\text{OTf})(\text{THF})$ (7).....	28
Figure S14. Solid-state molecular structure for $(^{\text{AdF}}\text{L})\text{Cr}(\text{NMes})(\text{THF})$ (8)	29

Figure S15. Characteristic image of the X-ray diffraction data for 8	30
Computational Methods	31
Geometry Optimized Structures	31
Table S3. Optimized geometry coordinates for (^{AdF} L)Cr(NMes)(THF) (8)	31
Table S4. Optimized geometry coordinates for (^{AdF} L)Cr(NMes)Cl (6).....	35
Table S5. Optimized geometry coordinates for (^{AdF} L)Cr(NMes)(OTf)(THF) (7).....	39
References	43

General Considerations

All manipulations of metal complexes were carried out in the absence of water and dioxygen using standard Schlenk techniques, or in an MBraun inert atmosphere drybox under a dinitrogen atmosphere. All glassware was oven dried overnight and cooled in an evacuated antechamber prior to use in the drybox. Benzene, hexanes, toluene, and tetrahydrofuran were dried over 4 Å molecular sieves (Strem) prior to use. Chloroform-*d* was purchased from Cambridge Isotope Labs and used as received. Benzene-*d*₆ was purchased from Cambridge Isotope Labs and was degassed and stored over 4 Å molecular sieves prior to use. Compounds 2,4,6-trimethylaniline, sodium azide, sodium nitrite, tetrabutylammonium chloride, thallium triflate, silver triflate, graphite, and potassium were purchased from Aldrich. Compounds 2,4,6-trimethylphenyl azide, potassium graphite, 2-adamantyl pyrrole and chromium bistriflate were prepared according to published procedures.¹⁻⁴ Celite® 545 (*J. T. Baker*) was dried in a Schlenk flask for 24 h under dynamic vacuum while heating to at least 150 °C prior to use in a drybox. Silica gel 32-63 μ (AIC, Framingham, MA) was used as received.

Characterization and Physical Measurements

¹H, ¹³C, ¹⁹F and were recorded on Varian Unity/Inova 500 MHz- spectrometers. ¹H and ¹³C NMR chemical shifts are reported relative to SiMe₄ using the chemical shift of residual solvent peaks as reference. ¹⁹F NMR chemical shifts are reported relative to an external standard of boron trifluoride diethyl etherate.

High-resolution mass spectrometry was performed on a Bruker microTOFII ESI LCMS or Bruker Maxis Impact LC-q-TOF Mass Spectrometer.

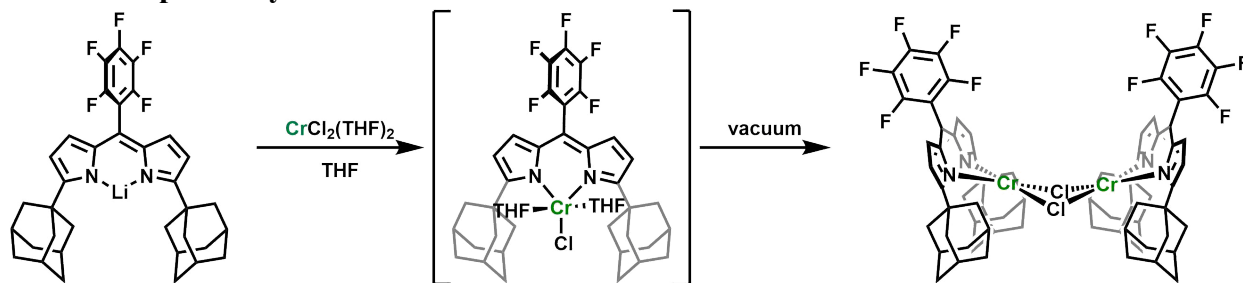
Elemental analysis was carried out using PerkinElmer 2400 CHNS/O Series II System.

EPR spectra were obtained on a Bruker EleXsys E-500 CW-EPR spectrometer. Spectra were measured as frozen toluene or 2-methyltetrahydrofuran glasses at a microwave power of 0.6325–2 mW. Spectral simulations and fitting incorporating spin state and rhombicity were performed using VisualRhomb and EasySpin.⁵⁻⁶

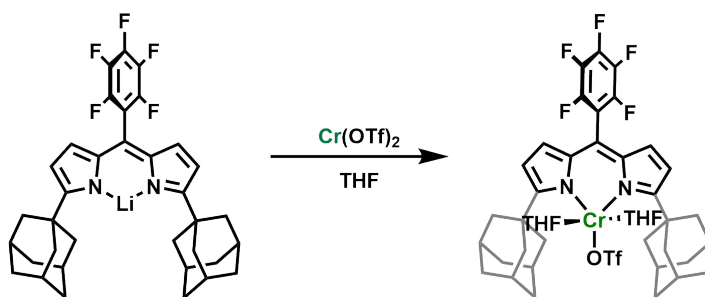
UV/Visible spectra were recorded on a Varian Cary 50 UV/Visible spectra using quartz cuvettes and a scan rate of 600 nm/min. Extinction coefficients were determined from four concentrations per sample, and were extracted from a linear regression fit of the absorbance vs. concentration.

Electrochemical experiments were carried out using a CH Instruments CHI660C Electrochemical Workstation. The supporting electrolyte was 0.1 M ($n\text{Bu}_4\text{N}$)(PF₆) in tetrahydrofuran. A glassy carbon working electrode, platinum wire counter electrode, and reference electrode were used. The concentration of each analyte was ~1 mM. Each scan was referenced internally to the potential for Fc/Fc⁺.

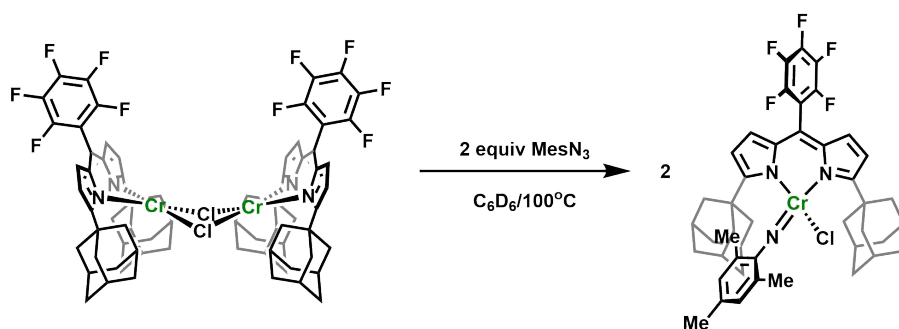
Metal Complexes Synthesis



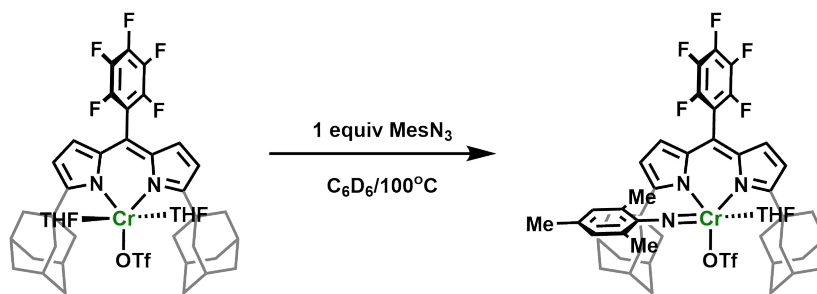
[(^{AdF}L)CrCl]₂ (2): A suspension of CrCl₂(THF)₂ (0.907 g, 3.42 mmol, 1.00 equiv) in 5 mL THF was frozen in a 20 mL scintillation vial. A solution of (^{AdF}L)Li (2.00 g, 3.42 mmol, 1.00 equiv) in 14 mL THF was added to the frozen suspension. The mixture was allowed to warm up to room temperature and stir for 10 min, during which the solution turned from dark yellow to dark orange. The solvent was removed *in vacuo*, which caused a color change from orange to deep pink. The pink solid was collected in benzene and lyophilized, washed with 20 mL of hexanes, filtered through a Celite plug, and lyophilized again to afford [(^{AdF}L)CrCl]₂ as a dark pink microcrystalline powder (1.93 g, 85%). Crystals suitable for X-ray diffraction were grown from a benzene solution at room temperature. ¹H NMR (500 MHz, C₆D₆): δ ppm −8.81, −38.60; ¹⁹F NMR (470 MHz, C₆D₆) δ ppm −106.22, −130.61, −151.83, −155.12, −162.82. ¹H NMR (500 MHz, THF): δ ppm 19.07, −6.11; ¹⁹F NMR (470 MHz, THF) δ ppm −143.10, −157.39, −164.73. Anal. Calc. for C₇₀H₆₈Cl₂Cr₂F₁₀N₄: C 63.21, H 5.15, N 4.21; Found C 63.57, H 5.27, N 4.42.



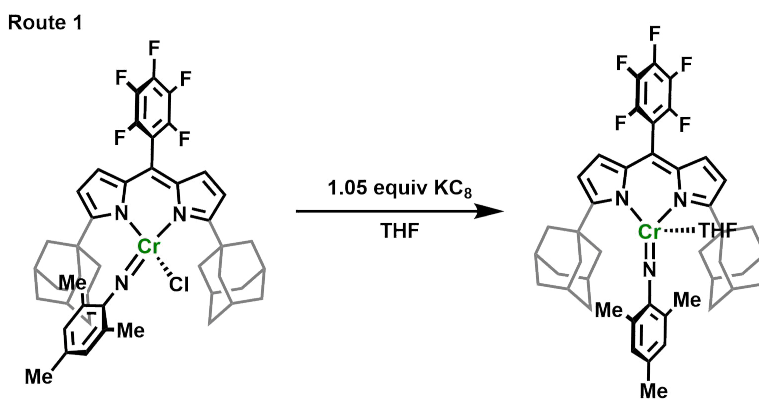
(^{Ad^F}L)Cr(OTf)(THF)₂ (3): A suspension of Cr(OTf)₂ (1.20 g, 3.42 mmol, 1.00 equiv) in 5 mL THF was frozen. A solution of (^{Ad^F}L)Li (2.00 g, 3.42 mmol, 1.00 equiv) in 14 mL THF was added to the frozen suspension. The mixture was allowed to warm up to room temperature and stirred for 20 min, during which the solution turned from dark yellow to dark orange. The solvent was removed *in vacuo*. The orange solid was collected in benzene and lyophilized. The resulting solid was dissolved in a minimal amount of 100:1 hexanes: THF mixture and stored at −35°C overnight to afford (^{Ad^F}L)Cr(OTf)(THF)₂ as orange needle-shaped crystals (1.67 g, 53%). This compound exhibits no ¹H NMR resonances. ¹⁹F NMR (470 MHz, THF) δ ppm −144.86, −156.89, −164.62. The compound loses one of its bound THF molecules upon lyophilization. Anal. Calc. for C₄₀H₄₂CrF₈N₂O₄S: C 56.53, H 4.86, N 3.30; Found C 56.84, H 4.64, N 3.48.



(^{Ad^F}L)Cr(NMes)Cl (6): A solution of [(^{Ad^F}L)CrCl]₂ (**1**) (0.200 g, 0.150 mmol, 1.00 equiv) and mesityl azide (48.5 mg, 0.300 mmol, 2.00 equiv) in 3 mL of C₆D₆ was added to a *J*-Young tube. The mixture was heated to 100°C overnight, during which the solution changed color from deep pink to deep maroon. The solvent was removed *in vacuo*. The solid residue was dissolved in 15 mL of hexanes and stored at −35°C overnight to give (^{Ad^F}L)Cr(NMes)Cl (0.197 g, 82%) as black needle-shaped crystals suitable for X-ray diffraction. ¹H NMR (500 MHz, C₆D₆): δ ppm 11.10, 8.37, −3.02, −9.59, −39.45, −48.94, −53.82, −82.80; ¹⁹F NMR (470 MHz, C₆D₆) δ ppm −141.88, −152.32, −161.28. Anal. Calc. for C₄₄H₄₅ClCrF₅N₃: C 66.20, H 5.68, N 5.26; Found C 65.94, H 5.62, N 5.65.

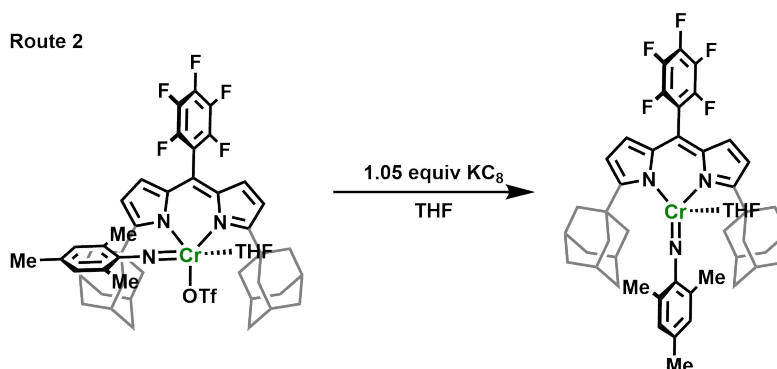


(^{AdF}L)Cr(NMes)(OTf)(THF) (7): A solution of (^{AdF}L)Cr(OTf)(THF)₂ (**2**) (0.200 g, 0.217 mmol, 1.00 equiv) and MesN₃ (35.0 mg, 0.217 mmol, 1.00 equiv) in 3 mL of C₆D₆ was added to a *J*-Young tube. The mixture was heated to 100 °C overnight, during which the solution changed color from deep pink to deep marron. The solvent was removed *in vacuo*. The solid residue was dissolved in 15 mL of hexanes and stored at −35 °C overnight to give (^{AdF}L)Cr(NMes)(OTf)(THF) (76.9 mg, 36%) as dark yellow plate-shaped crystals suitable for X-ray diffraction. ¹H NMR (500 MHz, C₆D₆): δ ppm 4.57, 3.47, −7.14, −60.30, −72.05, −118.00; ¹⁹F NMR (470 MHz, C₆D₆) δ ppm −48.16, −142.71, −152.24, −161.63. Anal. Calc. for C₄₉H₅₂CrF₈N₃O₄S: C 59.81, H 5.43, N 4.27; Found C 60.21, H 5.03, N 4.26.

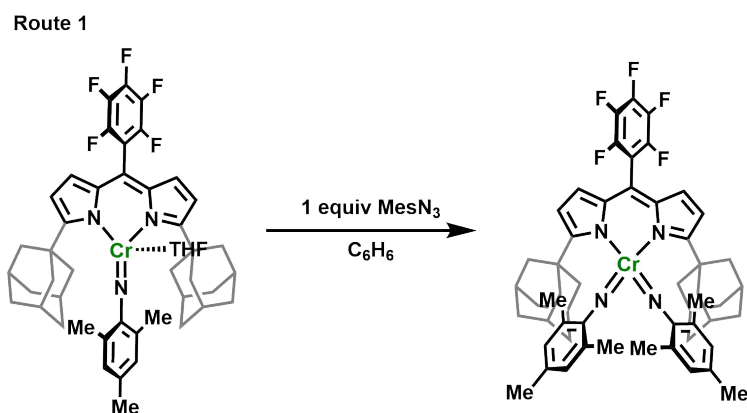


(^{AdF}L)Cr(NMes)(THF) (8, Route 1): A solution of (^{AdF}L)CrCl(NMes) (**5**) (50.0 mg, 0.0626 mmol, 1.00 equiv) in 5 mL of THF cooled till frozen using the cold well. Potassium graphite (8.9 mg, 0.066 mmol, 1.05 equiv) was added in one portion as soon as the solution started stirring, causing a color change from deep maroon to pink. The solution was allowed to stir for 3 min before it was filtered through a Celite plug. The solvent was removed *in vacuo*. The solid residue was dissolved in benzene and lyophilized. The resulting powder was dissolved in 1 mL of THF, transferred to a 4 mL shell vial which was placed in a 20 mL scintillation vial containing 10 mL

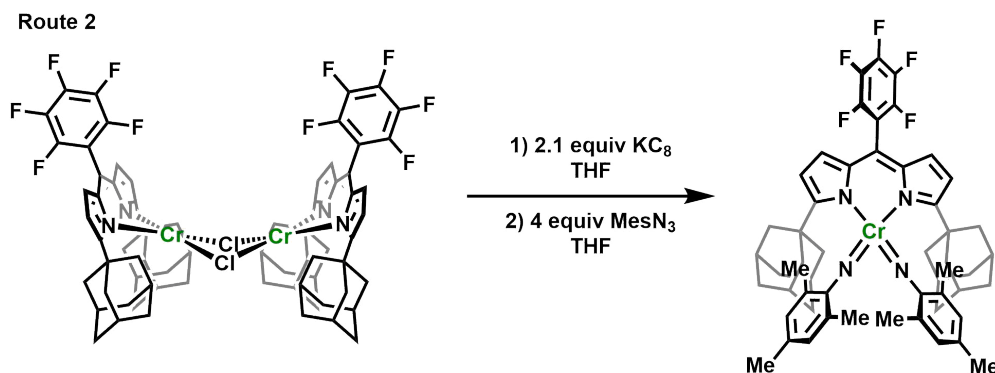
of hexanes and stored at -35°C to give $(^{\text{AdF}}\text{L})\text{Cr}(\text{NMes})(\text{THF})$ (29.8 mg, 57%) as pink plate-shaped crystals suitable for X-ray diffraction.



$(^{\text{AdF}}\text{L})\text{Cr}(\text{NMes})(\text{THF})$ (8, Route 2): A solution of $(^{\text{AdF}}\text{L})\text{Cr}(\text{OTf})(\text{NMes})(\text{THF})$ (7) (50.0 mg, 0.0543 mmol, 1.00 equiv) in 5 mL of THF was frozen in the cold well. Potassium graphite (7.7 mg, 0.057 mmol, 1.05 equiv) was added in one portion as soon as the solution started stirring, causing a color change from deep maroon to pink. The solution was allowed to stir for 3 min before it was filtered through a Celite plug. The solvent was removed *in vacuo*. The solid residue was collected in benzene and lyophilized. The resulting powder was dissolved in 1 mL of THF. The solution was transferred to a 4 mL shell vial which was placed in a 20 mL scintillation vial filled with 10 mL of hexanes and stored at -35°C to give $(^{\text{AdF}}\text{L})\text{Cr}(\text{NMes})(\text{THF})$ (18.8 mg, 36%) as pink plate-shaped crystals suitable for X-ray diffraction. ^1H NMR (500 MHz, C_6D_6): δ ppm 18.69, 10.51, 9.07, -18.38 , -65.13 , -67.92 , -107.64 ; ^{19}F NMR (470 MHz, C_6D_6) δ ppm -145.75 , -153.71 , -162.38 . Anal. Calc. for $\text{C}_{48}\text{H}_{52}\text{CrF}_5\text{N}_3\text{O}$: C 69.05, H 6.40, N 5.03; Found C 69.27, H 6.58, N 4.81.



(^{Ad^F}L)Cr(NMes)₂ (5, Route 1): To a solution of (^{Ad^F}L)Cr(NMes)(THF) (**8**) (30.0 mg, 0.0360 mmol, 1.00 equiv) in 3 mL of benzene, a solution of MesN₃ (5.8 mg, 0.036 mmol, 1.00 equiv) in 2 mL benzene was added dropwise. The solution was lyophilized, and the solid residue was dissolved in 3 mL of hexanes. The solution was stored at −35°C overnight to yield (^{Ad^F}L)Cr(NMes)₂ (20.6 mg, 64%) as pink block-shaped crystals suitable for X-ray diffraction.



(^{Ad^F}L)Cr(NMes)₂ (5, Route 2): A solution of [(^{Ad^F}L)CrCl]₂ (**1**) (50.0 mg, 0.0470 mmol, 1.00 equiv) in 5 mL of THF was frozen in the cold well. Potassium graphite (10.7 mg, 0.0790 mmol, 2.10 equiv) was added in one portion as soon as the solution started stirring, causing a color change from orange to deep purple. The solution was left stirring for 2 min before it was filtered through a Celite plug and frozen again using the cold well. A solution of MesN₃ (24.2 mg, 0.150 mmol, 4.00 equiv) in 2 mL of THF was added to the frozen solution. The mixture was allowed to warm up to room temperature and stir for an additional 5 min before the solvent was removed *in vacuo*. The solid residue was collected in benzene and lyophilized. The resulting powder was re-dissolved in benzene, filtered through a Celite plug, and the filtrate lyophilized to yield a pink, microcrystalline powder. The powder was dissolved in 5 mL of hexanes and stored at −35°C to afford (^{Ad^F}L)Cr(NMes)₂ (37.1 mg, 55%) as pink block-shaped crystals suitable for X-ray diffraction. This compound exhibits no ¹H NMR resonances. ¹⁹F NMR (470 MHz, C₆D₆) δ ppm −140.59, −152.97, −161.50. Anal. Calc. for C₅₃H₅₆CrF₅N₄: C 71.04, H 6.30, N 6.25; Found C 71.22, H 6.58, N 6.12.

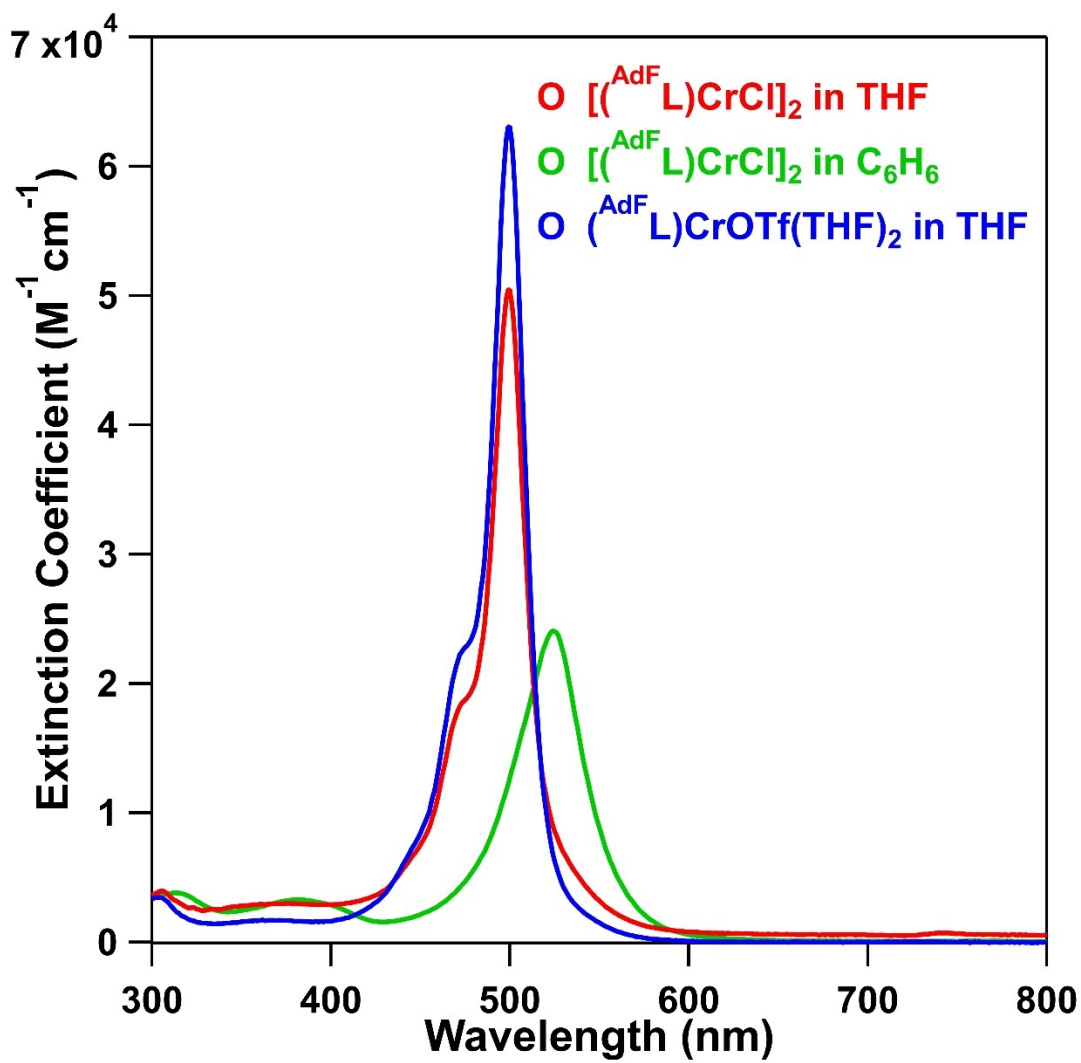


Figure S1. UV-Vis Spectrum of [(^{AdF}L)CrCl]₂ (**2**) and (^{AdF}L)Cr(OTf)(THF)₂ (**3**)

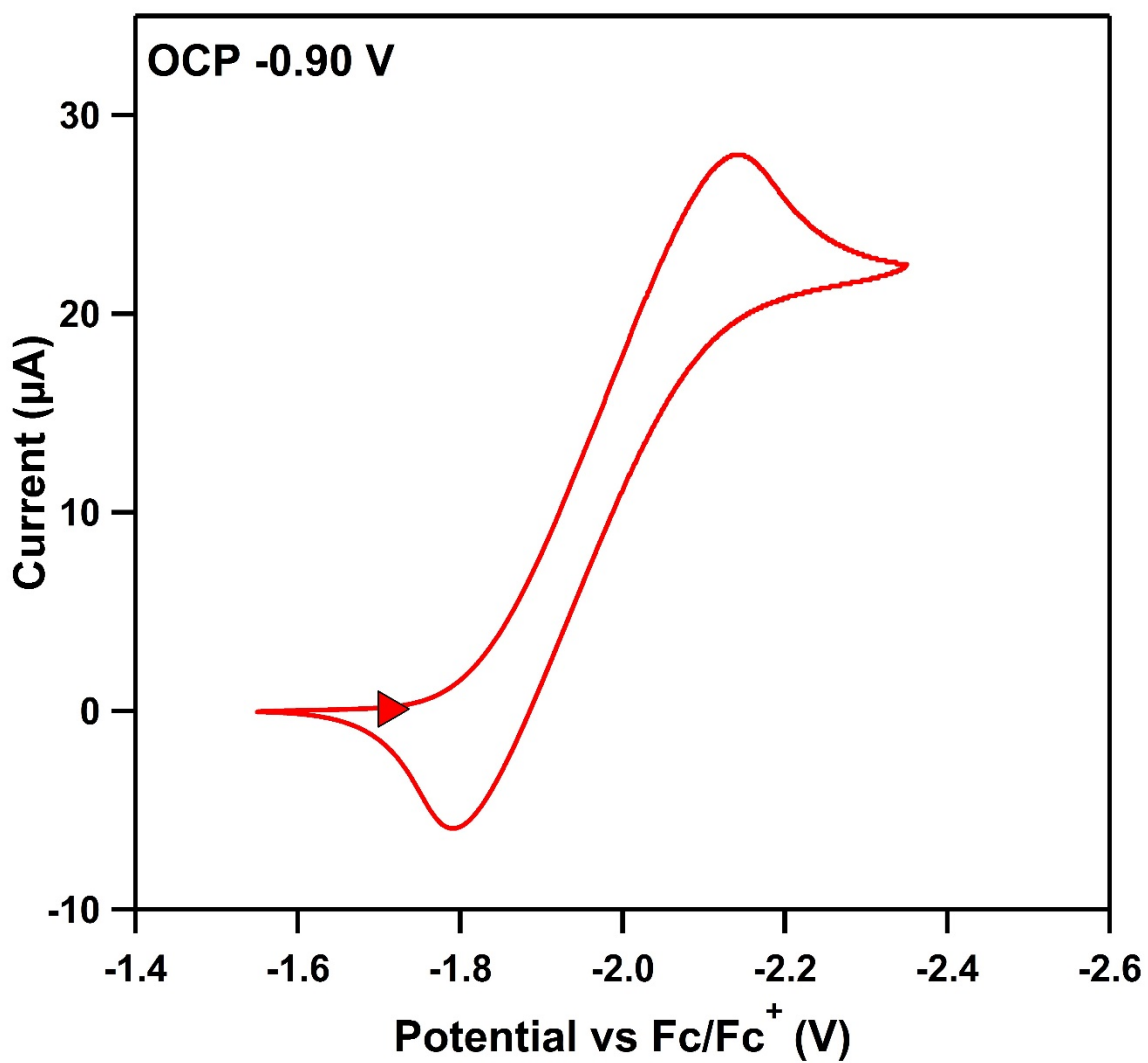


Figure S2. Cyclic voltammogram of $[(^{\text{AdF}}\text{L})\text{CrCl}]_2$ (**2**). The data were obtained in THF at 25 °C, with 0.1 M (*n*Bu₄N)(PF₆) as supporting electrolyte and a scan rate of 20 mV/s.

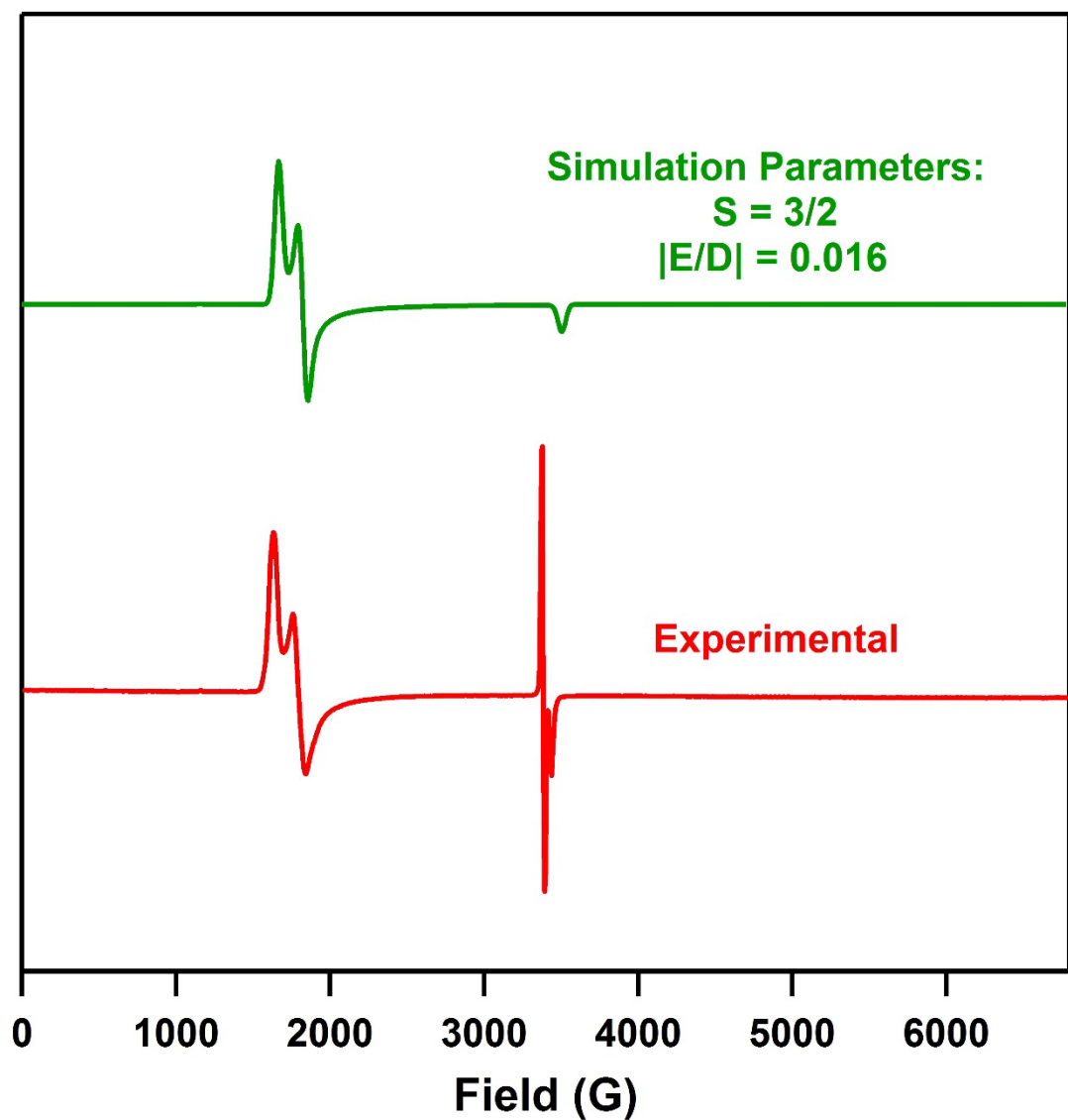


Figure S3. Frozen 2-methyl tetrahydrofuran EPR spectrum of transiently stable chromium (I) species **4** at 77 K. The green trace represents a simulation with VisualRhombos⁵ resulting from spin state $S = 3/2$ and $|E/D| = 0.016$ as input.

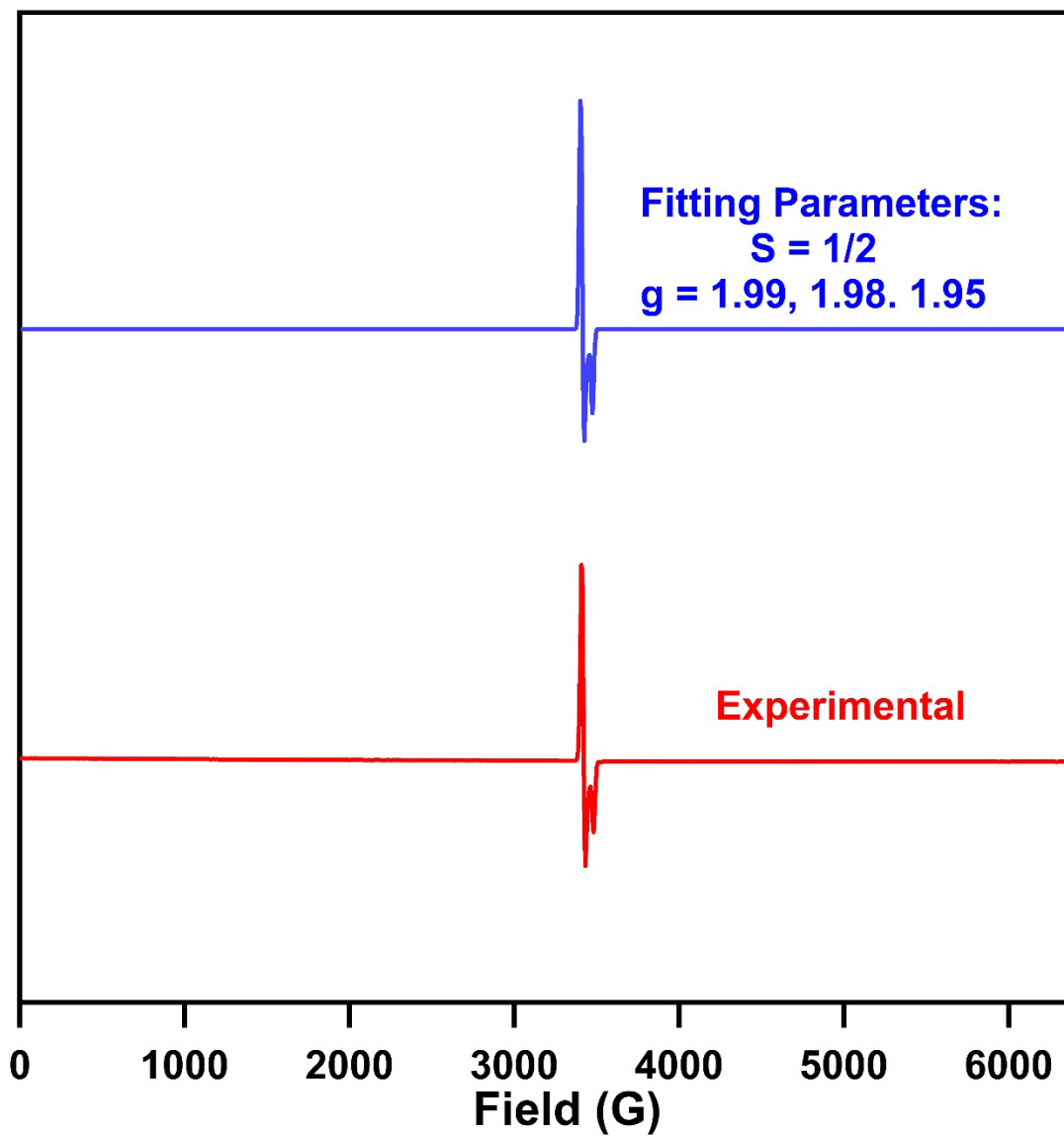


Figure S4a. Full field frozen toluene EPR spectrum of (^{AdF}L)Cr(NMes)₂ (**5**) at 77 K. The blue trace represents a fitted spectrum with EasySpin⁶ with spin state $S = 1/2$ and $g = [1.99, 1.98, 1.95]$ as output.

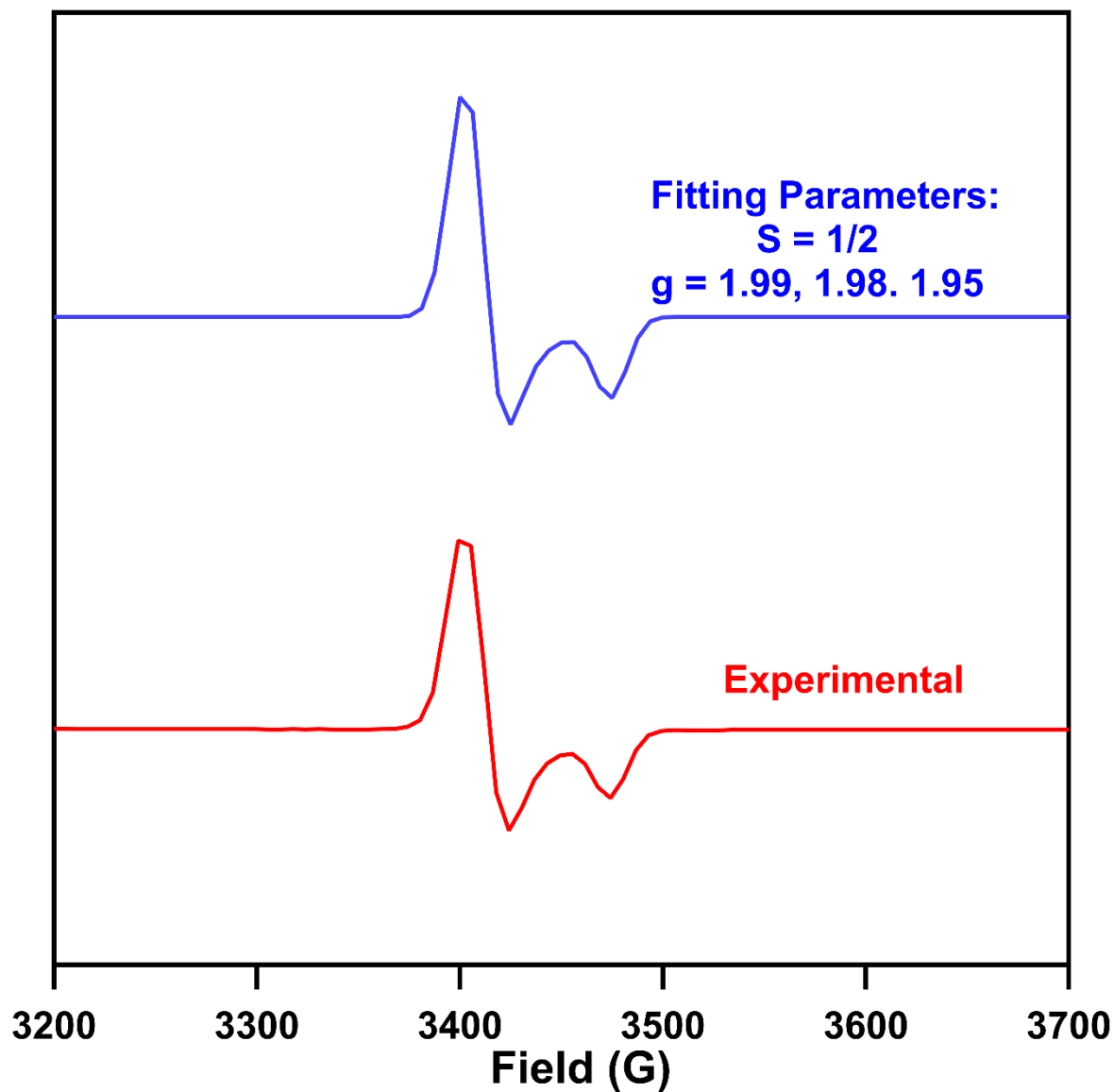


Figure S4b. Zoomed-in frozen toluene EPR spectrum of (^{Ad^F}L)Cr(NMes)₂ (**5**) at 77 K.

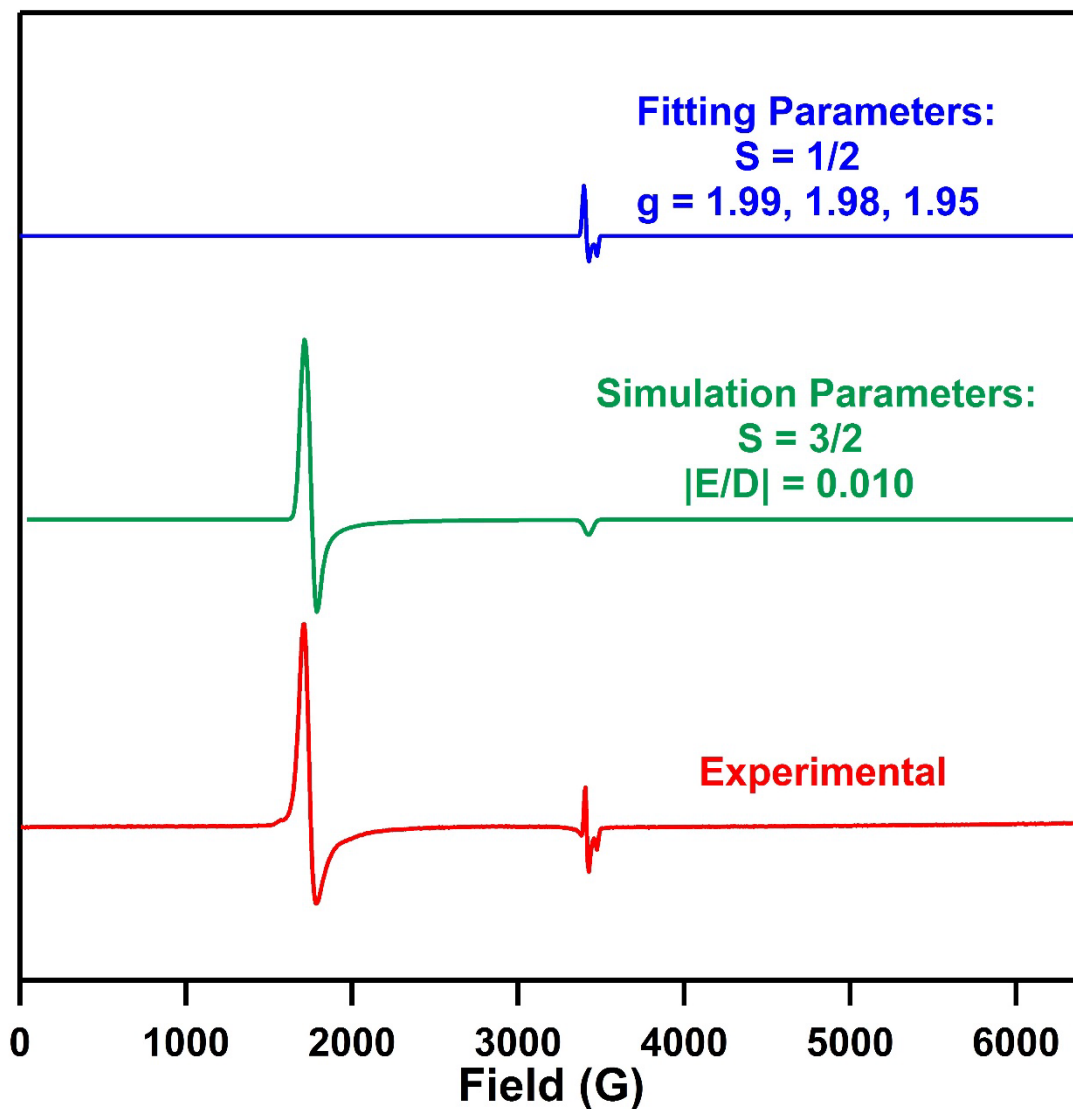


Figure S5a. Frozen toluene EPR spectrum of (^{AdF}L)Cr(NMes)(THF) (**8**) at 77 K. The blue trace represents a fitted spectrum with EasySpin⁶ with spin state $S = 1/2$ and $g = [1.99, 1.98, 1.95]$ as output. The green trace represents a simulation with VisualRhomb⁵ resulting from spin state $S = 3/2$ and $|E/D| = 0.010$ as input.

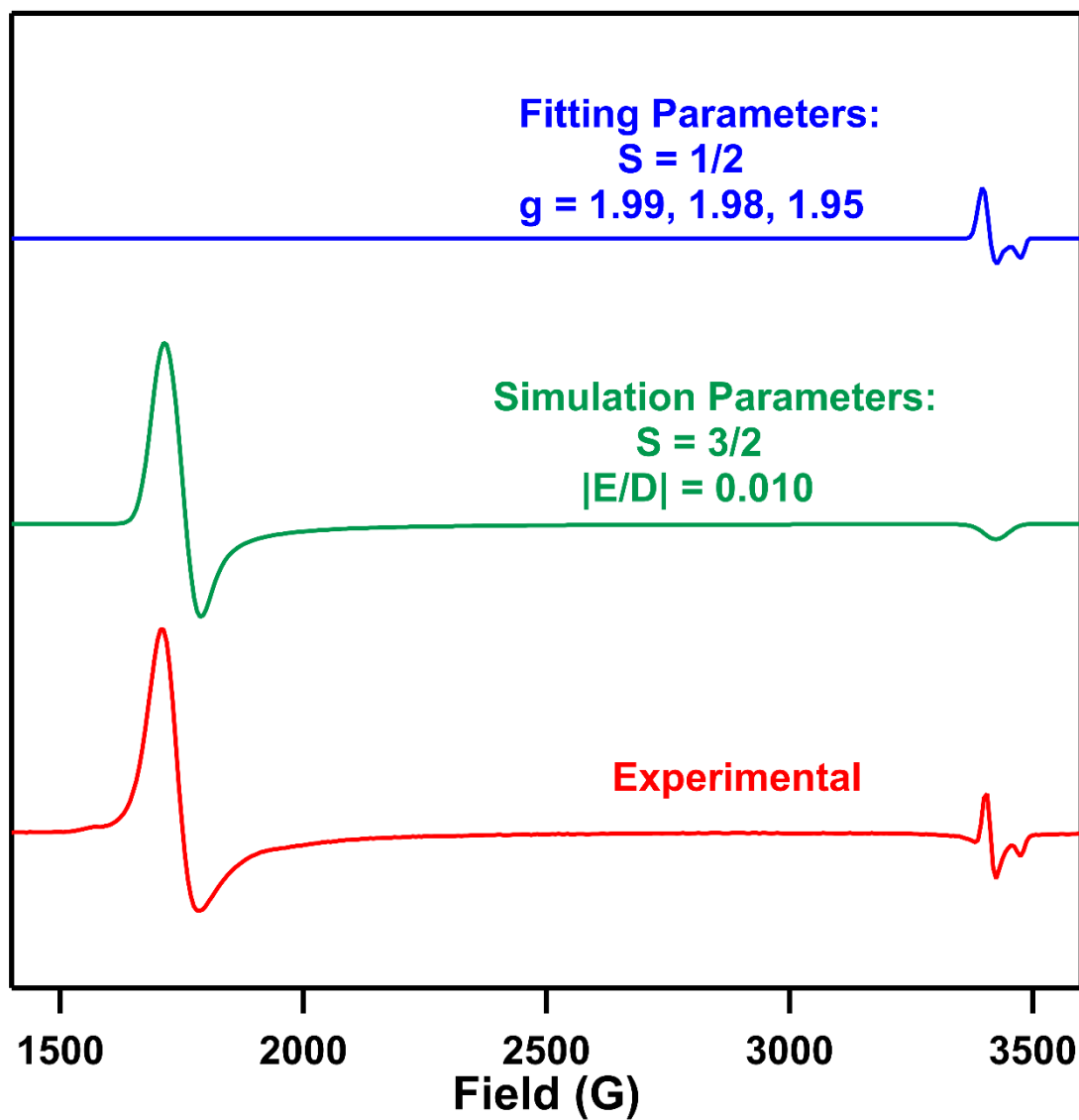


Figure S5b. Zoomed-in frozen toluene EPR spectrum of (^{AdF}L)Cr(NMes)(THF) (**8**) at 77 K.

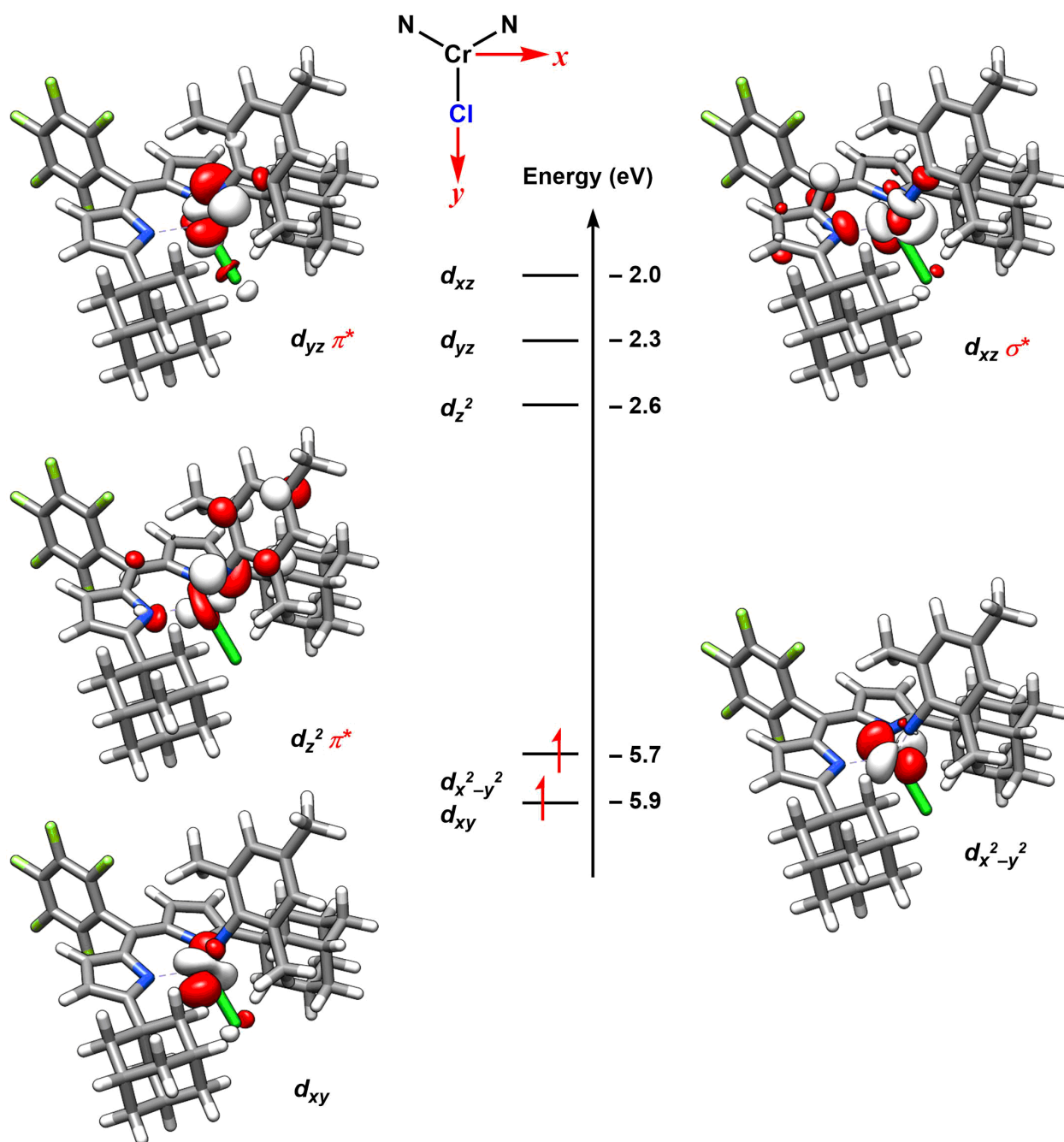


Figure S6. Frontier molecular orbital diagram showing metal d-orbitals for **6**. [UKS B3LYP /def2-svp (C, H, F) and def2-tzvp (Cr, N)]. Z-axis is defined as the Cr–N_{im} bond vector.

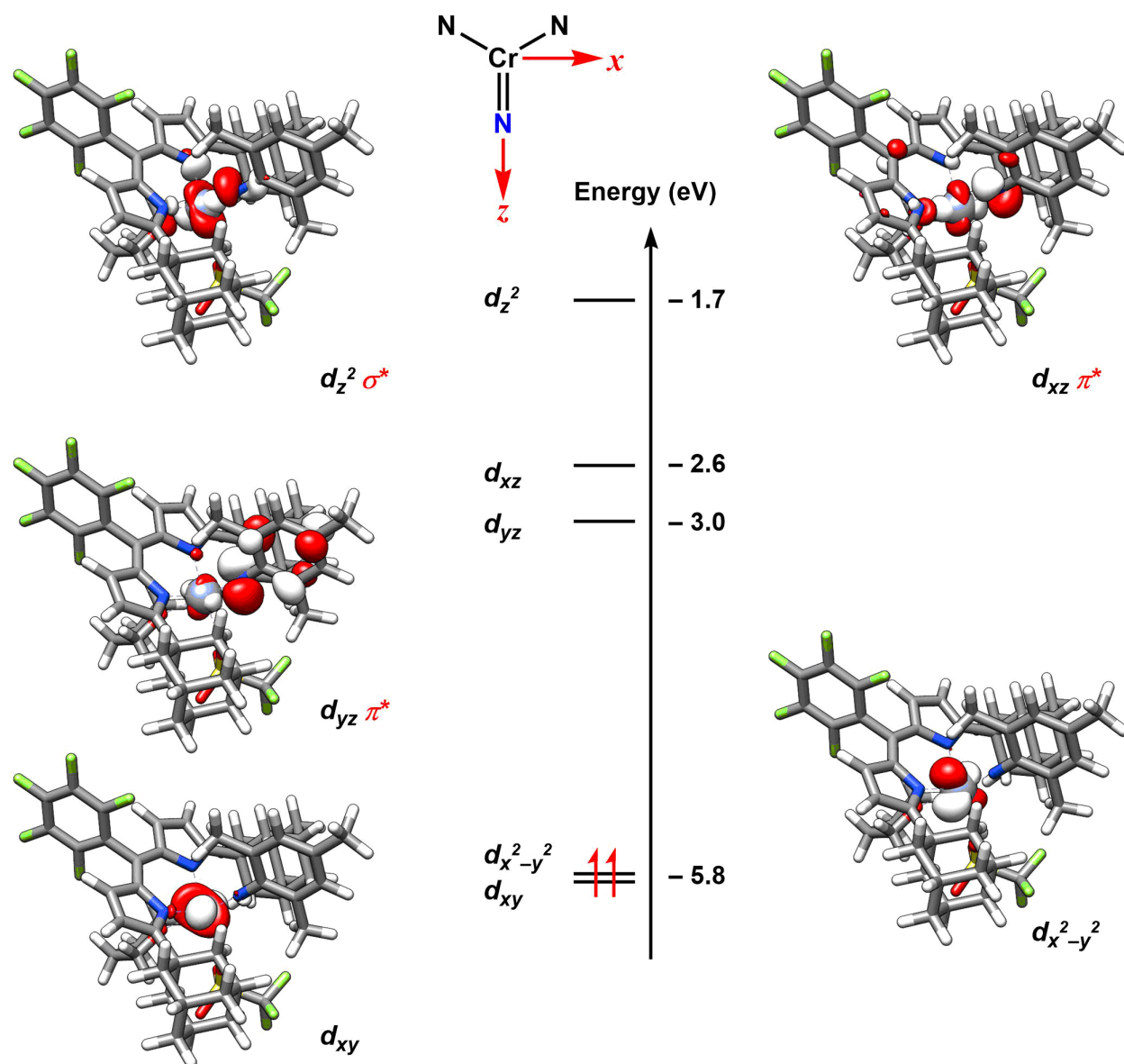


Figure S7. Frontier molecular orbital diagram showing metal d-orbitals for **7**. [UKS B3LYP /def2-svp (C, H, F) and def2-tzvp (Cr, N)]. Z-axis is defined as the Cr–N_{im} bond vector.

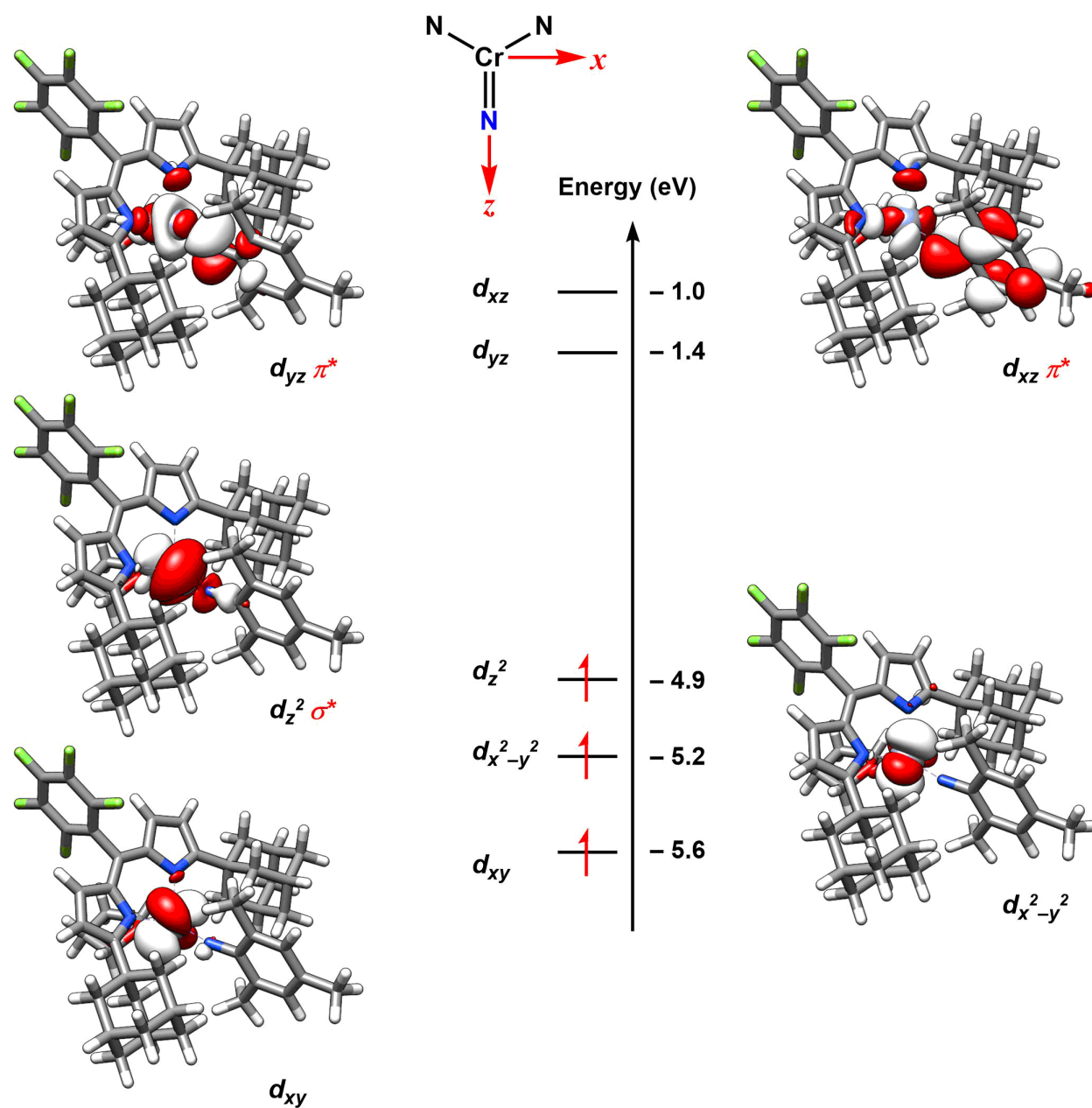


Figure S8. Frontier molecular orbital diagram showing metal d-orbitals for **8**. [UKS B3LYP /def2-svp (C, H, F) and def2-tzvp (Cr, N)]. Z-axis is defined as the Cr–N_{im} bond vector.

Table S1. Bond Metrics Comparison Between DFT Optimized and Solid-State Molecular Structures

	DFT	Solid-State	$ \Delta $
<hr/> (^{AdF} L)Cr(NMes)Cl (6) (Å) <hr/>			
Cr–N _L	2.053	2.024(6)	0.029
Cr–N _L	2.021	2.004(5)	0.017
Cr–N _{im}	1.651	1.641(4)	0.010
Cr–Cl	2.260	2.257(2)	0.003
<hr/> (^{AdF} L)Cr(NMes)(OTf)(THF) (7) (Å) <hr/>			
Cr–N _L	2.107	2.055	0.007
Cr–N _L	2.068	2.025	0.007
Cr–N _{im}	1.708	1.665	0.008
Cr–OTf	2.071	2.030	0.008
Cr–THF	2.254	2.177	0.007
<hr/> (^{AdF} L)Cr(NMes)(THF) (8) (Å) <hr/>			
Cr–N _L	2.098	2.101(2)	0.003
Cr–N _L	2.098	2.100(3)	0.002
Cr–N _{im}	1.713	1.709(3)	0.004
Cr–THF	2.277	2.140(10)	0.137

X-Ray Diffraction Techniques

Structures of **2**, **3**, and **5-8** were collected on a Bruker three-circle platform goniometer equipped with an Apex II CCD and an Oxford cryostream cooling device. Radiation was from a graphite fine focus sealed tube Mo K α (0.7107 Å) or Cu K α (1.5418 Å) source. Crystals were mounted on a cryoloop or glass fiber pin using Paratone N oil. Structures were collected at 100 K. Data were collected as a series of ϕ and/or ω scans.

Data were integrated using SAINT and scaled with either a numerical or multi-scan absorption correction using SADABS. The structures were solved by intrinsic phasing, direct methods or Patterson maps using SHELXS-2014 and refined against F^2 on all data by full matrix least squares with SHELXL-2014.⁷⁻⁸ All non-hydrogen atoms were refined anisotropically. Hydrogen atoms were placed at idealized positions and refined using a riding model. The isotropic displacement parameters of all hydrogen atoms were constrained to be 1.2 times the parameter of the atoms they were linked to (1.5 times for methyl groups). Further details on structures are noted below.

[(^{AdF}L)CrCl]₂ (2): (CCDC:1967093) The structure was solved in the monoclinic space group $P\bar{1}$ with four molecules per unit cell and two molecules in the asymmetric unit. The asymmetric unit also contains two benzene solvent molecules. One adamantyl group, one chloride group and one pentafluorophenyl group are disordered and are modeled with similarity restraints and constraints.

(^{AdF}L)Cr(OTf)(THF)₂ (3): (CCDC:1967094) The structure was solved in the triclinic space group $P\bar{1}$ with four molecules per unit cell and two molecules in the asymmetric unit. Two coordinated THF molecules, one adamantyl group and two triflate groups are disordered and are modeled with similarity restraints and constraints.

(^{AdF}L)Cr(NMes)₂ (5): (CCDC:1967095) The structure was solved in the orthorhombic space group $Pbca$ with eight molecules per unit cell and one molecule in the asymmetric unit. The asymmetric unit also contains one hexanes molecule.

(^{AdF}L)Cr (NMes)Cl (6): (CCDC:1967096) The structure was solved in the monoclinic space group $P2_1/c$ with four molecules per unit cell and one molecule in the asymmetric unit.

(^{AdF}L)Cr (NMe_s)(OTf)(THF) (7): (CCDC:1967097) The structure was solved in the monoclinic space group $P2_1$ with four molecules per unit cell and two molecules in the asymmetric unit. Both molecules display full molecule disorder and are modeled with similarity restraints and constraints. Residue electron density from disordered solvent molecules are squeezed out using solvent mask.

(^{AdF}L)Cr(NMe_s)(THF) (8): (CCDC:1967098) The structure was solved in the monoclinic space group $P\bar{1}$ with two molecules per unit cell and one molecule in the asymmetric unit. The asymmetric unit also contains two disordered hexane molecules with partial occupancy. The disordered solvent molecules are modeled with similarity restraints and constraints.

Table S2. X-ray diffraction experimental details

	$[(^{\text{AdF}}\text{L})\text{CrCl}]_2$ (2)	$(^{\text{AdF}}\text{L})\text{Cr}(\text{OTf})(\text{THF})_2$ (3)	$(^{\text{AdF}}\text{L})\text{Cr}(\text{NMes})_2$ (5)
Moiety			
Formula	$2\text{C}_{38}\text{H}_{37}\text{ClCrF}_5\text{N}_2$	$\text{C}_{44}\text{H}_{50}\text{CrF}_8\text{N}_2\text{O}_5\text{S}$	$\text{C}_{59}\text{H}_{70}\text{CrF}_5\text{N}_4$
FW	1408.29	922.92	982.19
λ (nm)	0.71073	1.54178	0.71073
T (K)	100(2)	100(2)	100(2)
Crystal System	Triclinic	Triclinic	Orthorhombic
Space Group (Z)	$P\bar{1}$ (2)	$P\bar{1}$ (2)	$Pbca$ (8)
a (Å)	15.8112(15)	11.3653(4)	15.3902(8)
b (Å)	18.2465(18)	17.4031(7)	22.0785(8)
c (Å)	23.607(2)	21.1322(5)	29.9364(15)
α (°)	78.927(3)	93.966(3)	90
β (°)	87.544(3)	102.004(2)	90
γ (°)	81.311(3)	96.269(3)	90
Volume (Å³)	6606.4(11)	4045.7(2)	10172.2(8)
Calc. ρ (mg/m³)	1.416	1.515	1.283
μ (mm⁻¹)	0.486	3.570	0.286
Crystal Size (mm)	0.25×0.18×0.04	0.18×0.04×0.03	0.19×0.12×0.05
Reflections	62138	48836	61358
Completeness (to 2θ)	99.0%	93.9%	99.0%
	25.091	66.595	25.092
GOF on F²	1.031	1.026	1.017
R1, $wR2^a$			
$[I > 2\sigma(I)]$	0.0664, 0.1872	0.0710, 0.2022	0.0697, 0.1586

^a $R1 = \sum ||F_o| - |F_c|| / \sum |F_o|$, $wR2 = \{\sum [w(F_o^2 - F_c^2)^2] / \sum [w(F_o^2)^2]\}^{1/2}$

Table S2. X-ray diffraction experimental details (continued)

	(^{AdF} L)Cr(NMes)Cl (6)	(^{AdF} L)Cr(NMes)(OTf)(THF) (7)	(^{AdF} L)Cr(NMes)(THF) (8)
Moiety	C ₄₄ H ₄₅ ClCrF ₅ N ₃	2C ₄₉ H ₅₈ CrF ₈ N ₃ O ₄ S	C ₄₈ H ₅₃ CrF ₅ N ₃ O; C ₆ H ₁₄
Formula			
FW	798.28	1968.00	921.10
λ (nm)	0.71073	0.71073	1.54178
T (K)	100(2)	100(2)	100(2)
Crystal System	Monoclinic	Monoclinic	Triclinic
Space Group (Z)	<i>P</i> 2 ₁ / <i>c</i> (4)	<i>P</i> 2 ₁ (2)	<i>P</i> $\bar{1}$ (2)
<i>a</i> (Å)	18.229(3)	17.0256(12)	11.4314(4)
<i>b</i> (Å)	20.427(3)	17.8637(13)	13.7772(5)
<i>c</i> (Å)	10.3857(18)	17.9461(12)	15.3492(6)
α (°)	90	90	104.593(2)
β (°)	105.421(4)	112.061(2)	91.816(2)
γ (°)	90	90	93.766(3)
Volume (Å³)	3728.0(11)	5058.5(6)	2331.43(15)
Calc. ρ (mg/m³)	1.422	1.292	1.312
μ (mm⁻¹)	0.441	0.341	2.532
Crystal Size (mm)	0.20×0.18×0.04	0.17×0.02×0.02	0.22×0.16×0.05
Reflections	25545	107586	29059
Completeness (to 2θ)	99.5%	98.9%	93.9%
	25.074	25.146	66.858
GOF on F²	1.044	1.018	1.029
R1, wR2^a			
[<i>I</i> > 2σ(<i>I</i>)]	0.0965, 0.1538	0.0671, 0.1661	0.0573, 0.1596

^a $R1 = \sum ||F_o| - |F_c|| / \sum |F_o|$, $wR2 = \{\sum [w(F_o^2 - F_c^2)^2] / \sum [w(F_o^2)^2]\}^{1/2}$

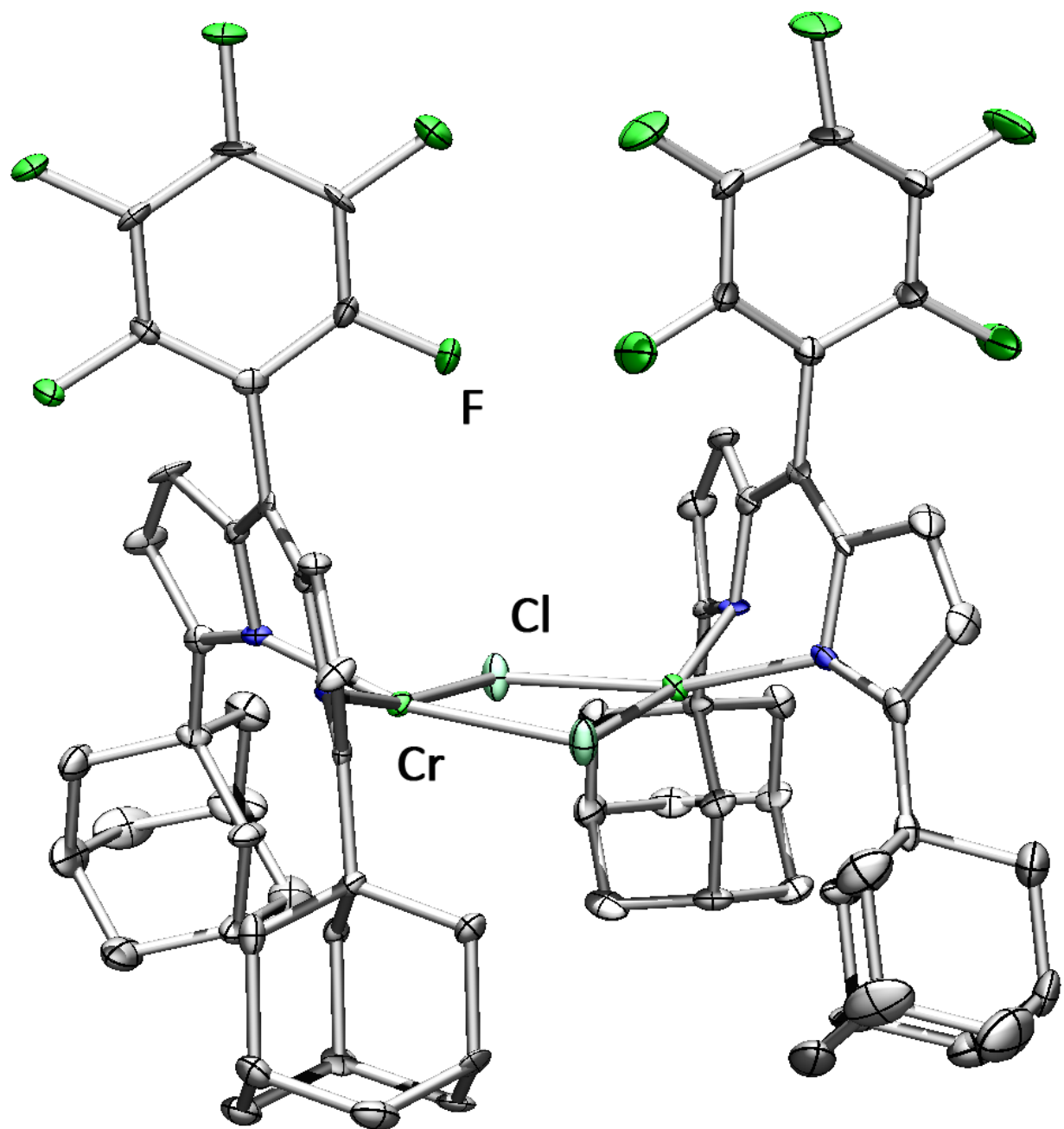


Figure S9. Solid-state molecular structure for $[(^{AdF}L)CrCl]_2$ (**2**) with thermal ellipsoids at 50% probability level. Hydrogens and benzene solvent in the unit cell were omitted for clarity.

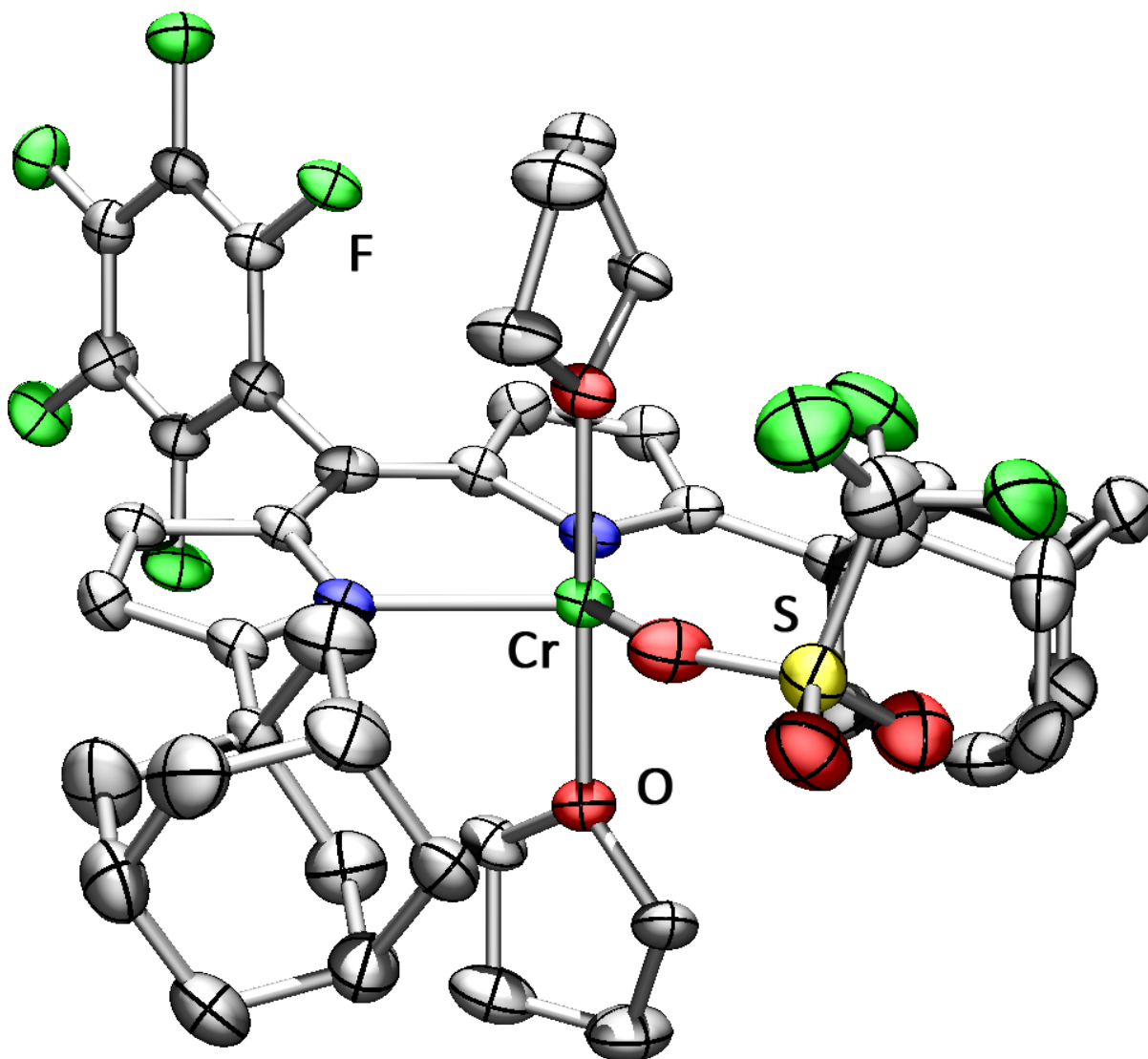


Figure S10. Solid-state molecular structure for $(^{AdF}L)Cr(OTf)(THF)_2$ (**3**) with thermal ellipsoids at 50% probability level. Hydrogens were omitted for clarity.

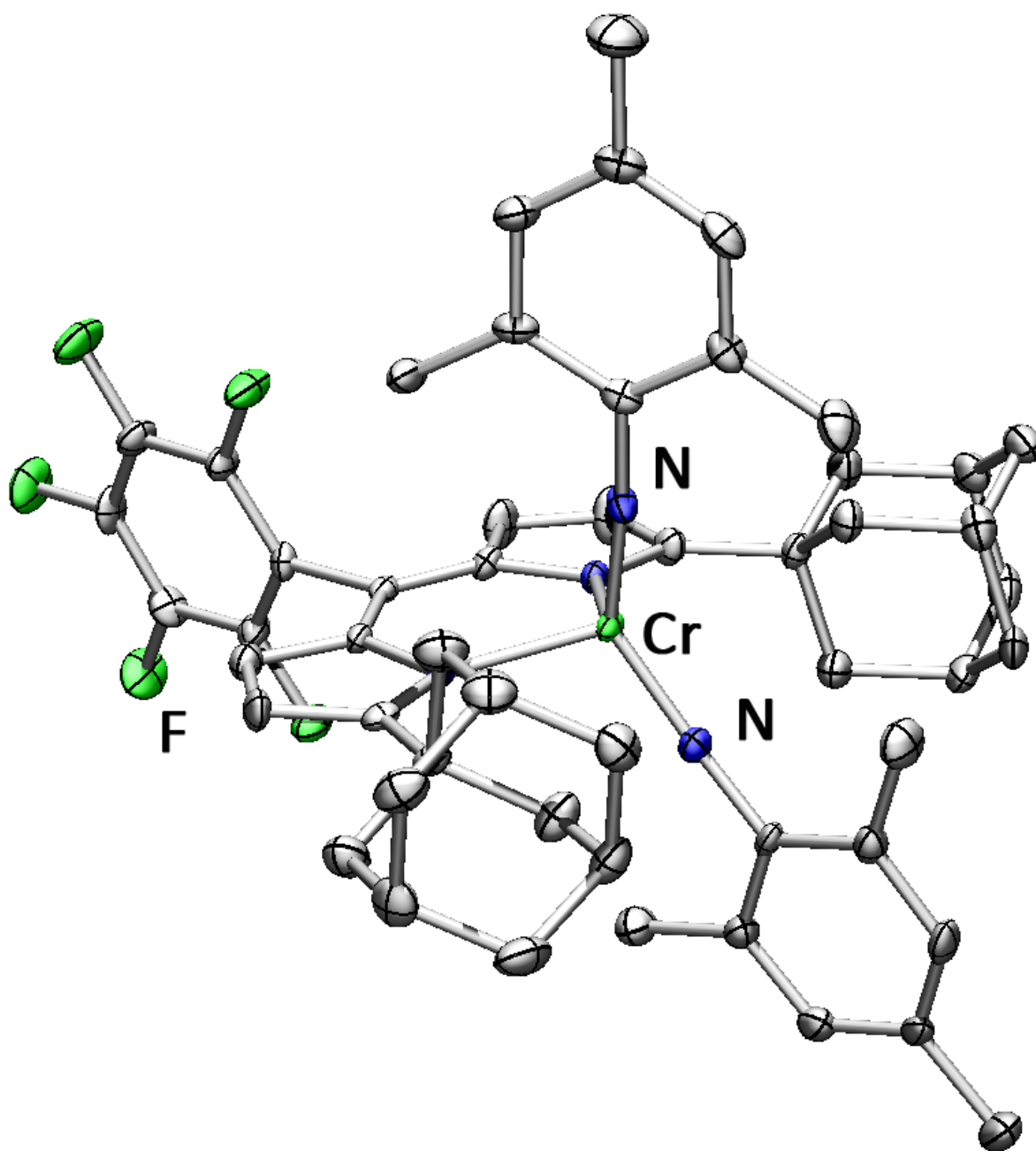


Figure S11. Solid-state molecular structure for $(^{AdF}L)Cr(NMes)_2$ (**5**) with thermal ellipsoids at 50% probability level. Hydrogens were omitted for clarity.

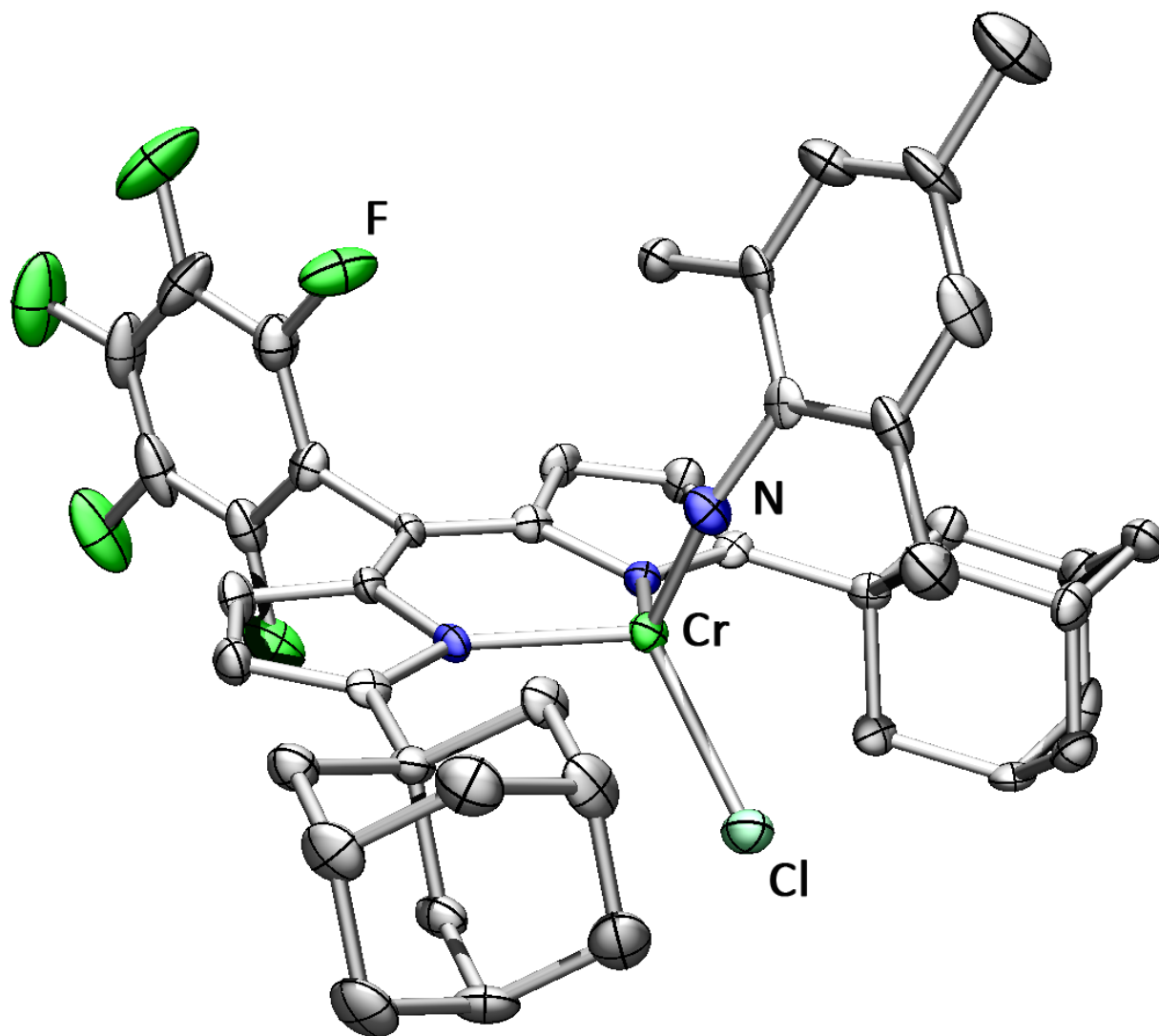


Figure S12. Solid-state molecular structure for $(^{AdF}L)Cr(NMes)Cl$ (**6**) with thermal ellipsoids at 50% probability level. Hydrogens were omitted for clarity.

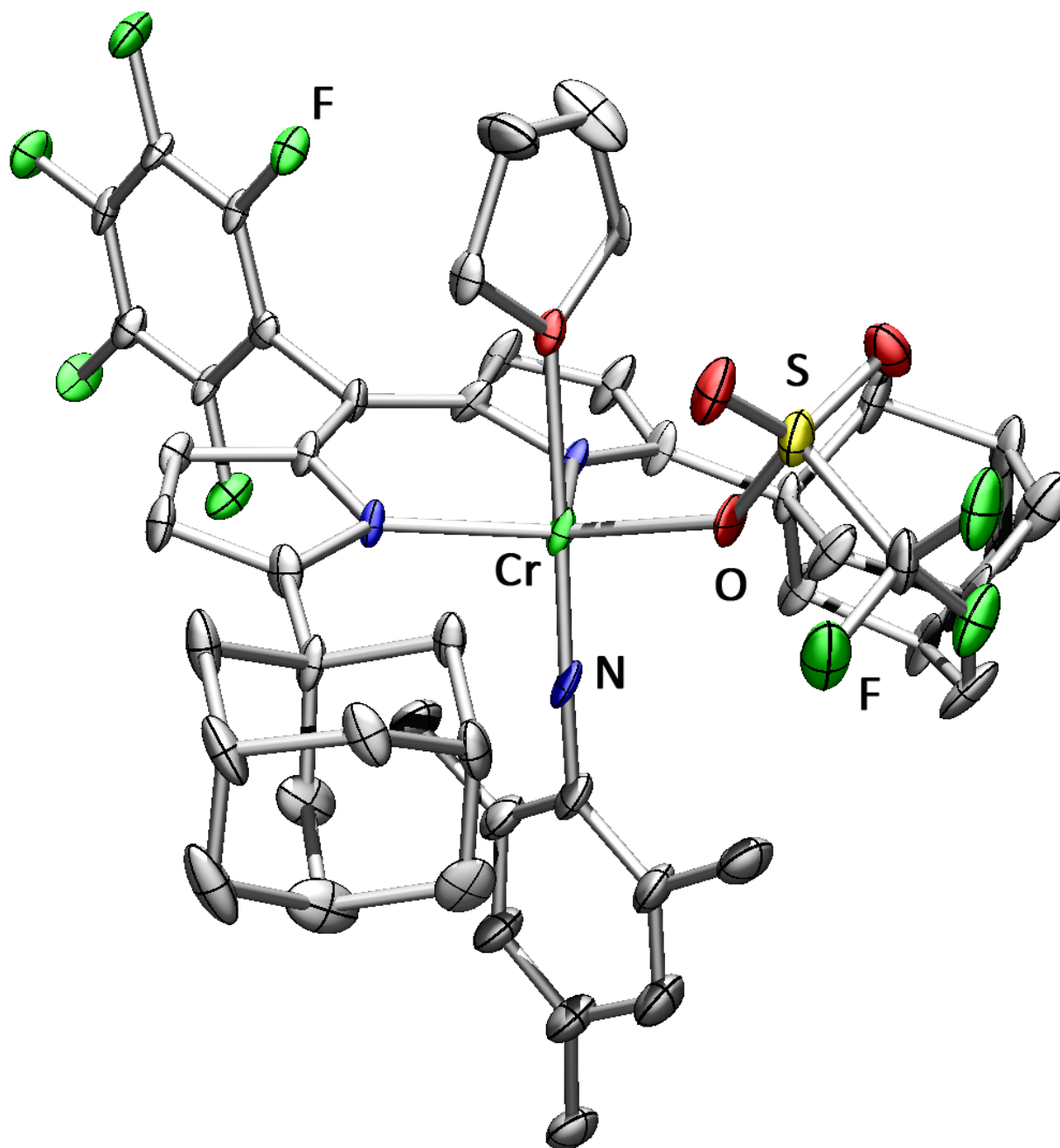


Figure S13. Solid-state molecular structure for $(^{AdF}L)Cr(NMes)(OTf)(THF)$ (7) with thermal ellipsoids at 50% probability level. Hydrogens, disordered fragments, and benzene solvent in the unit cell were omitted for clarity.

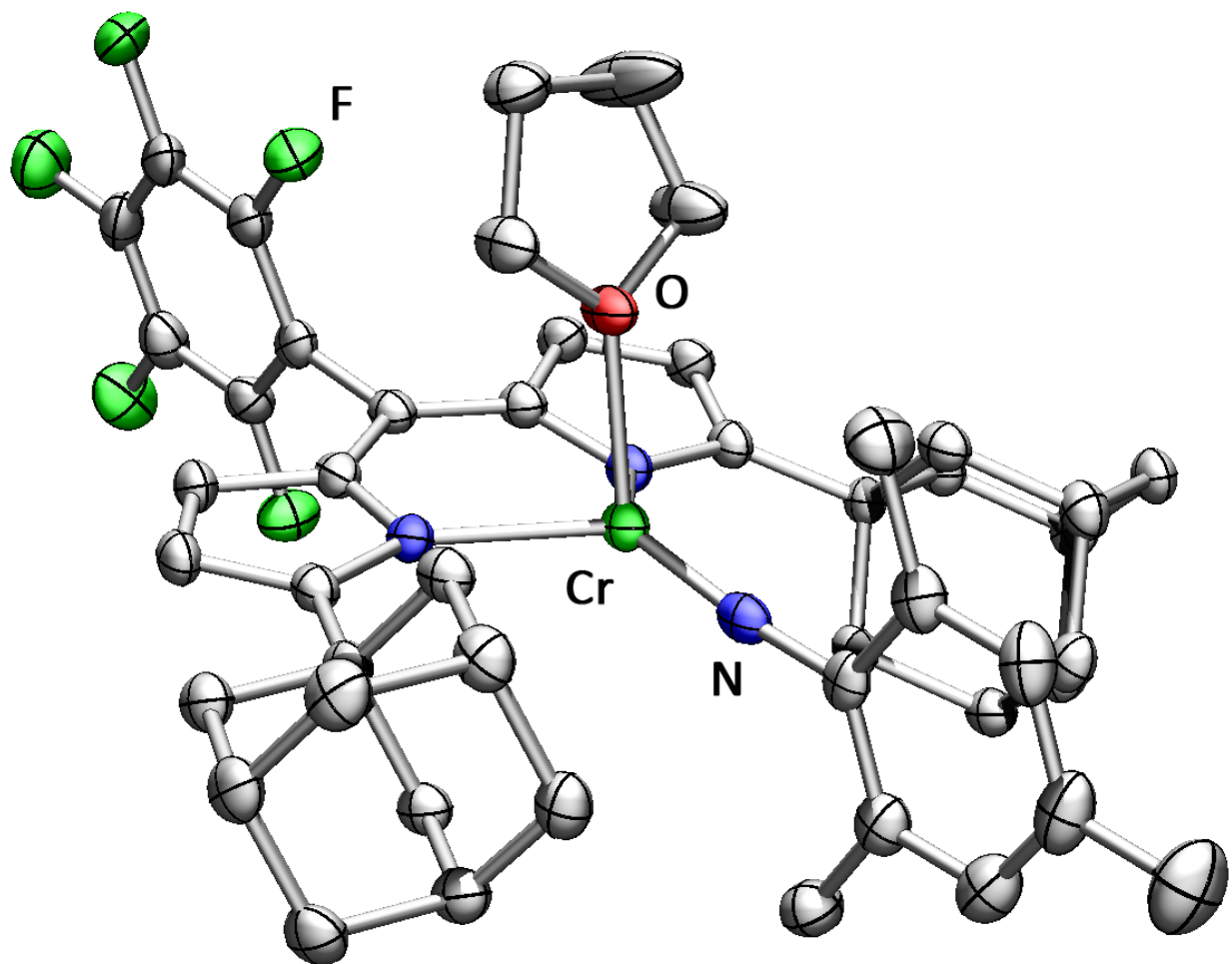


Figure S14. Solid-state molecular structure for (^{AdF}L)Cr(NMes)(THF) (**8**) with thermal ellipsoids at 50% probability level. Hydrogens were omitted for clarity.

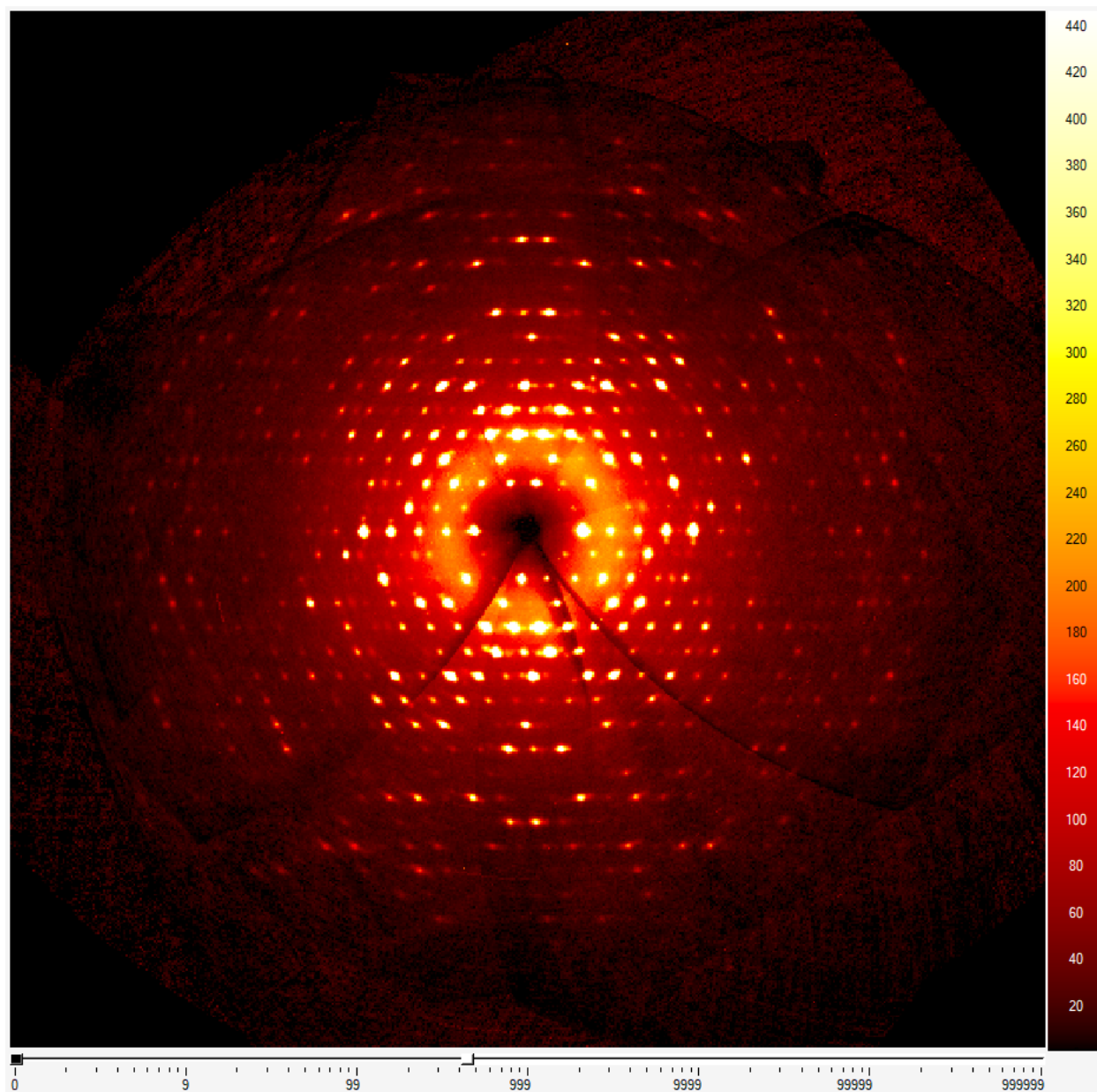


Figure S15. Characteristic image of the X-ray diffraction data for $(^{\text{AdF}}\text{L})\text{Cr}(\text{NMes})(\text{OTf})(\text{thf})$ **7**, illustrating the presence of diffuse scattering along the Bragg peaks due to the inherent disorder of the system. The crystal structures have been modeled to account for this disorder, which gives rise to elongated thermal parameters.

Computational Methods

Computations were carried out using the Gaussian 09 program package. The B3LYP functional was used with the def2-TZVP (Cr, N, F, S, O, Cl), def2-SVP (C,H) basis sets and the W06 density fitting function of Ahlrichs and co-workers.⁹⁻¹⁴ Frequency calculations were performed at the same level of theory in order to confirm the optimized structures were minima on the potential energy surfaces.¹⁵

Geometry Optimized Structures

Table S3. Optimized geometry coordinates for (^{Ad^F}L)Cr(NMes)(THF) (**8**)

Cr	0.5764665	-0.0001316	0.5064893
F	-3.7271133	0.000977	-3.0396691
F	-4.6614158	-0.0004713	1.6113127
F	-6.3794609	0.0011409	-3.5668249
F	-7.3105278	-0.0002935	1.073612
O	-0.4788218	-0.00041	2.523693
F	-8.1861386	0.0005135	-1.5168012
N	-0.7052078	-1.5710445	-0.0317207
N	-0.7050132	1.5710717	-0.0314054
N	2.2258311	-0.0001187	0.0436858
C	-2.0495359	-1.2794795	-0.2944722
C	-2.6262149	0.0001607	-0.3990828
C	-2.0494045	1.2797116	-0.2940975
C	-0.5776813	2.9187349	-0.0555611
C	3.3947153	-0.0000569	-0.6640622
C	-0.5780133	-2.918715	-0.0561631
C	0.4211314	5.2296955	0.1363428
H	-0.0828678	5.5195225	-0.7999607
H	-0.2710563	5.4688214	0.961832
C	-4.1032635	0.0002661	-0.6972271
C	0.7170597	3.703401	0.1224076
C	-2.7618	2.5056222	-0.4687312

H	-3.8217672	2.6074178	-0.6885431
C	-1.8466921	-3.5228724	-0.3208729
H	-2.0482647	-4.5863887	-0.4000727
C	1.7149016	6.0516622	0.2853328
H	1.4544979	7.124087	0.2937819
C	2.9824985	4.2505244	-0.9162192
H	3.6455553	4.0209853	-1.7671779
C	2.7501016	-4.176357	1.5872201
H	3.2466038	-3.8953889	2.5322735
C	-2.7620564	-2.5052698	-0.4694178
H	-3.8220196	-2.606904	-0.6893268
C	1.6887699	3.4251576	-1.0616472
H	1.9315399	2.3550745	-1.0879511
H	1.1827061	3.6716603	-2.0108819
C	-4.584133	0.0006669	-2.01219
C	1.68859	-3.4252621	-1.0619085
H	1.1826914	-3.6716048	-2.0112729
H	1.9314772	-2.3551998	-1.0880368
C	-1.8463156	3.5230902	-0.3200402
H	-2.0477688	4.5866453	-0.3990207
C	1.4484687	-3.3605158	1.4501663
H	1.6843818	-2.2848628	1.4809886
H	0.782658	-3.579619	2.3022317
C	0.7166134	-3.7035388	0.1219178
C	2.750899	4.1758453	1.5873441
H	3.2475584	3.8947167	2.5322668
C	3.6850555	3.8703618	0.4007217
H	3.9554077	2.8030074	0.3871654
H	4.6258339	4.4382643	0.5066316
C	3.4114478	0.0000628	-2.0909258
C	1.4491432	3.3601651	1.4504734

H	0.7835449	3.5793003	2.3026979
H	1.6849231	2.2844785	1.4811624
C	2.4168117	5.6782947	1.6035885
H	3.3382908	6.2732699	1.7273444
H	1.7647858	5.9166165	2.4624816
C	-5.055431	-0.0000566	0.3276737
C	2.6476094	5.7526933	-0.903189
H	3.5722937	6.3501885	-0.8220118
H	2.1607787	6.0447556	-1.8501353
C	4.6370036	-0.0001431	0.0448028
C	0.420528	-5.2298052	0.1356263
H	-0.2718546	-5.4689526	0.960946
H	-0.0833097	-5.5194742	-0.8008129
C	-5.9521361	0.0007553	-2.3007069
C	1.7141804	-6.0519236	0.2847865
H	1.4536666	-7.1243231	0.2930648
C	4.6439799	0.0000954	-2.755682
H	4.6450813	0.0001711	-3.8505747
C	3.6845335	-3.8708422	0.4008194
H	3.9549968	-2.8035132	0.387437
H	4.6252309	-4.4388539	0.5068578
C	2.9822046	-4.2507808	-0.9163081
H	3.6454619	-4.0212165	-1.7671037
C	2.6471619	-5.7529178	-0.9035106
H	2.1604964	-6.0448258	-1.8505896
H	3.5717697	-6.3505145	-0.8222101
C	-6.4284371	0.0000228	0.0685348
C	2.4158534	-5.6787729	1.6032301
H	1.7636227	-5.917121	2.4619604
H	3.3372451	-6.2738567	1.7271131
C	2.1256328	0.0001041	-2.878138

H	1.503705	-0.8792674	-2.6475723
H	2.326363	0.0003208	-3.9595534
H	1.5035538	0.8792765	-2.6472408
C	5.8684085	0.000024	-2.0760087
C	-0.7992975	-1.1546113	3.3280688
H	0.0439418	-1.3522752	4.0143245
H	-0.9183053	-2.0069863	2.6507569
C	-2.077516	-0.7752739	4.0872316
H	-2.9643245	-1.1602863	3.5653161
H	-2.0766419	-1.1988418	5.102258
C	4.6407116	-0.0002918	1.5520828
H	4.1145184	0.8790883	1.9578058
H	5.667715	-0.0002778	1.9464997
H	4.1146167	-0.8798123	1.9576325
C	-6.8777603	0.0004352	-1.2541959
C	5.8341965	-0.000105	-0.6721354
H	6.7778179	-0.0001867	-0.1159623
C	7.184034	0.0001854	-2.816102
H	7.7922701	-0.8848452	-2.5614097
H	7.7913491	0.8862104	-2.5626285
H	7.0347062	-0.0006171	-3.9062936
C	-0.7983015	1.1537373	3.3285134
H	0.0447387	1.3499531	4.0154475
H	-0.9158603	2.0066639	2.6516521
C	-2.0774228	0.77541	4.0864798
H	-2.9634277	1.1599757	3.5628702
H	-2.0779074	1.200056	5.1010553

Table S4. Optimized geometry coordinates for (^{AdFL})Cr(NMes)Cl (**6**)

Cr	-0.7748918	0.2490844	-0.3210982
Cl	-2.1617865	0.5663351	-2.0765043
F	3.59721	-0.6618425	2.4026474
F	4.4326928	-0.1648295	-2.2385855
N	0.7160332	1.612517	-0.2776889
F	7.0742993	-0.5504764	-1.7993167
N	0.349358	-1.4145862	-0.7474518
F	7.9920414	-0.9924703	0.7358079
N	-1.4630187	0.2564698	1.1798215
F	6.2400483	-1.0456431	2.8324321
C	0.7546577	2.9710947	-0.2035002
C	0.0556504	-2.719278	-0.9989484
C	2.0239461	1.1455438	-0.0796275
C	-2.0935074	-0.1930205	2.3032352
C	2.0884497	3.3910665	0.0704539
H	2.423276	4.4170059	0.18164
C	-0.3892778	3.9370155	-0.4756509
C	-1.3064436	-3.2882819	-1.3615242
C	-1.2935797	-4.8396247	-1.2391743
H	-1.0292663	-5.131594	-0.208323
H	-0.521381	-5.2612996	-1.902219
C	-0.6631951	3.990233	-2.0122843
H	-0.9389757	2.9900783	-2.3757797
H	0.2642567	4.2828018	-2.5337068
C	-1.3510261	-0.8935339	3.2997098
C	2.2788969	-2.6546348	-0.5879725
H	3.323371	-2.9203368	-0.4447145
C	1.7258447	-1.346179	-0.4847205
C	2.4568926	-0.1876286	-0.1739991
C	1.2417866	-3.5041647	-0.9057792

H	1.311604	-4.5758406	-1.0612825
C	-2.4348531	-2.7619277	-0.4351067
H	-2.2009532	-3.0153529	0.6126221
H	-2.4983733	-1.6666602	-0.4973505
C	2.8753632	2.2628234	0.1505085
H	3.9470122	2.222669	0.3289975
C	-3.4869925	0.0535786	2.4843505
C	3.9271076	-0.4015982	0.067112
C	0.1163348	-1.164515	3.1082692
H	0.2949812	-1.8084143	2.2319007
H	0.5450698	-1.6617413	3.9897203
H	0.6792507	-0.2349066	2.9290262
C	-1.6549835	-2.945574	-2.8431432
H	-1.6634819	-1.8561366	-2.9825199
H	-0.866755	-3.3526693	-3.499458
C	-2.6582323	-5.4417195	-1.6261994
H	-2.6021158	-6.5389067	-1.5218882
C	-3.7991215	-3.3554822	-0.837134
H	-4.5741024	-2.9432578	-0.1687018
C	4.429597	-0.6292685	1.3535531
C	-4.1153822	-2.9736806	-2.2968129
H	-5.1031228	-3.3737148	-2.5851185
H	-4.1672595	-1.8776155	-2.4000738
C	-1.7049906	3.5598292	0.2523163
H	-2.0336575	2.560341	-0.056053
H	-1.5265807	3.5173194	1.3403442
C	-3.3864435	-1.0875454	4.6530131
C	4.8501552	-0.3803611	-0.9856979
C	-2.9820323	-5.0747135	-3.0867634
H	-3.950704	-5.5133992	-3.3829961
H	-2.2195231	-5.4984759	-3.7635025

C	-2.0170645	-1.3182671	4.4505952
H	-1.4471255	-1.8519304	5.2172439
C	-4.0968062	-0.4053625	3.6530016
H	-5.1671767	-0.2232831	3.7894397
C	-3.0245699	-3.5420681	-3.2256932
H	-3.2491318	-3.2679259	-4.2705762
C	0.0017863	5.374209	-0.0259003
H	0.2251811	5.3795099	1.0547819
H	0.9178431	5.6948474	-0.5467429
C	-2.8228002	4.5701836	-0.0723801
H	-3.7420687	4.260304	0.4541959
C	-3.7538346	-4.8871495	-0.6987099
H	-4.7328216	-5.3245652	-0.9608273
H	-3.5469489	-5.1699634	0.3482753
C	5.7920839	-0.8294715	1.5921895
C	-1.1186317	6.3835356	-0.3407611
H	-0.7974275	7.3838958	-0.0031955
C	-1.7882368	4.9975085	-2.3248996
H	-1.96512	5.0009014	-3.4140223
C	-4.2782446	0.7866508	1.4348116
H	-3.9013083	1.8121409	1.2964556
H	-5.3399664	0.847088	1.7131752
H	-4.2035121	0.2992382	0.4501354
C	-2.4075357	5.9757023	0.3935673
H	-3.2118639	6.7027289	0.1860515
H	-2.2428738	5.9833116	1.4853048
C	6.6892636	-0.8029629	0.5214862
C	-3.0774214	4.5779891	-1.5924071
H	-3.3961025	3.5776402	-1.9282585
H	-3.8955346	5.2782145	-1.8356957
C	6.2178786	-0.5771885	-0.7743732

C	-1.3718597	6.4050725	-1.860259
H	-0.460685	6.7293071	-2.3928456
H	-2.1612509	7.1371962	-2.1038178
C	-4.0689624	-1.5319728	5.9220349
H	-3.5810979	-2.4180256	6.3562044
H	-5.1291498	-1.7728698	5.7492129
H	-4.0378843	-0.7359934	6.6875254

Table S5. Optimized geometry coordinates for (^{AdF}L)Cr(NMes)(OTf)(THF) (**7**)

Cr	0.3858175	0.0489116	-0.24908
S	2.6202506	-0.3997154	-2.6714186
O	2.0539987	-0.5889219	-1.2994452
O	2.56852	-1.6047721	-3.4566893
O	2.2258862	0.8386651	-3.29396
C	4.4338138	-0.155206	-2.3017824
F	4.9366871	-1.1750691	-1.5874936
F	5.1142383	-0.0671881	-3.4508017
F	4.6321716	0.9790292	-1.6063527
F	-4.3890974	0.0165269	2.5400997
F	-7.0907083	-0.0441042	2.6394398
F	-8.5462517	-0.1773175	0.330413
F	-4.567922	-0.1870951	-2.1951706
F	-7.2686863	-0.2488262	-2.0853689
N	-0.8869132	-1.5861864	0.1329568
N	-0.9769856	1.5853113	-0.0088696
N	1.19391	0.3321487	1.2287646
O	-0.5808279	-0.0594335	-2.2827793
C	-0.9022658	1.104311	-3.1009039
H	-1.8413657	1.5398617	-2.7239293
H	-0.0867298	1.8265242	-2.993547
C	-0.8820281	-1.2862939	-3.0228141
H	0.0695068	-1.7790465	-3.2669424
H	-1.4765945	-1.9405775	-2.3737056
H	-0.0595038	0.5025604	-4.9973129
C	-1.6257046	-0.8319522	-4.2748255
H	-2.7091052	-0.7758082	-4.0834465
C	-1.0477545	0.5667104	-4.517271
H	-1.6964482	1.2038791	-5.1364845

H	-1.4621608	-1.520533	-5.1166476
C	0.7186149	0.2239098	3.6013662
C	1.6359687	0.3256695	2.5013169
C	3.0436949	0.4223902	2.7552063
C	3.4870538	0.4347657	4.0775563
H	4.5626958	0.4982834	4.2663699
C	2.6044806	0.3645149	5.1657561
C	-0.7421943	-2.9231811	0.3030143
C	-2.0307486	-3.535983	0.4089546
H	-2.226096	-4.5934284	0.552541
C	-2.9731677	-2.5406399	0.3109088
H	-4.0525982	-2.65554	0.3670806
C	-2.2638302	-1.3112618	0.1549857
C	-2.8811156	-0.0488012	0.1091783
C	-2.3346346	1.2463679	0.0522436
C	-3.101806	2.4494294	0.0729862
H	-4.1856479	2.5178139	0.119626
C	-0.7605962	0.1103403	3.3604719
H	-1.154487	0.9964906	2.8393035
H	-1.3060624	0.0006303	4.3078115
H	-0.9944838	-0.7548399	2.7220711
C	-2.2086771	3.494655	0.0267734
H	-2.4551919	4.5514794	0.0295038
C	4.0203844	0.4399995	1.6135882
H	4.0785186	-0.5474207	1.1276724
H	5.0293198	0.7077186	1.9573088
H	3.7160174	1.1439985	0.8279768
C	-0.8933025	2.9370156	-0.0206075
C	3.1058002	0.4178119	6.5856406
H	4.1907901	0.2465055	6.6411928
H	2.6056122	-0.3336113	7.2175154

H	2.9016055	1.4037386	7.0393929
C	-4.3871342	-0.0849288	0.1692989
C	-5.1624729	-0.1520868	-0.9934238
C	-6.5591307	-0.1843963	-0.9550052
C	-7.2138527	-0.1475687	0.2786774
C	-6.4676187	-0.0795092	1.4580991
C	-5.071906	-0.0486372	1.3897199
C	1.2284741	0.2579963	4.8966162
H	0.5266357	0.1956546	5.733854
C	0.5568665	-3.718297	0.3666413
C	1.661687	-3.0040927	1.1864846
C	0.2918605	-5.0993472	1.0378961
C	1.1047611	-3.9981688	-1.0663082
H	1.2924604	-2.7987272	2.2053248
H	1.9010755	-2.0370342	0.7288136
C	2.9444215	-3.8577236	1.2450084
H	-0.4623864	-5.6585609	0.4626461
H	-0.1210115	-4.9479564	2.0500096
C	1.5744091	-5.9478663	1.1076863
H	1.3214926	-3.0518808	-1.5795698
H	0.3320819	-4.5212716	-1.6556706
C	2.3881067	-4.8518499	-0.9984011
H	3.7057696	-3.3091747	1.8258742
C	2.6448607	-5.2043996	1.9248564
C	3.4614391	-4.1041036	-0.1853545
H	1.3349499	-6.9094063	1.5936789
C	2.0884919	-6.2016946	-0.3220736
H	2.7520795	-5.0175457	-2.026003
H	2.2902547	-5.0420179	2.9578851
H	3.563964	-5.8118213	1.9934005
H	3.705955	-3.1486711	-0.6728115

H	4.3924761	-4.6963812	-0.1543331
H	2.9990468	-6.8249355	-0.2951128
H	1.3348656	-6.7629858	-0.901949
C	0.3682313	3.7930741	-0.0178753
C	1.5413203	3.2004617	-0.8375603
C	0.0520347	5.1997853	-0.6096417
C	0.846951	4.003544	1.4532464
H	1.2403565	3.0602778	-1.8866373
H	1.8167246	2.2103646	-0.4490038
C	2.780069	4.117908	-0.7781814
H	-0.7546852	5.6805164	-0.0355072
H	-0.3112116	5.0917809	-1.6459181
C	1.2876972	6.1175883	-0.5681869
H	1.0878468	3.0293692	1.9050638
H	0.0235084	4.4373691	2.0455812
C	2.0798191	4.9295114	1.4981873
H	3.5889772	3.6472018	-1.3598512
C	2.4328188	5.4898454	-1.381044
C	3.2263133	4.3005615	0.6853076
H	1.0152226	7.0959192	-0.999895
C	1.7266197	6.3024132	0.8968611
H	2.3916242	5.052234	2.5496275
H	2.134219	5.3769376	-2.4374678
H	3.317693	6.1495097	-1.367788
H	3.5131212	3.3311009	1.1230545
H	4.1210771	4.9453666	0.7299382
H	2.59889	6.9763433	0.9515951
H	0.9183946	6.7789493	1.4789357

References

1. King, E. R.; Hennessy, E. T.; Betley, T. A., Catalytic C–H Bond Amination from High-Spin Iron Imido Complexes. *J. Am. Chem. Soc.* **2011**, *133*, 4917-4923.
2. Kwok, S. W.; Fotsing, J. R.; Fraser, R. J.; Rodionov, V. O.; Fokin, V. V., Transition-Metal-Free Catalytic Synthesis of 1,5-Diaryl-1,2,3-triazoles. *Org. Lett.* **2010**, *12*, 4217-4219.
3. Lalancette, J. M.; Rollin, G.; Dumas, P., Metals Intercalated in Graphite. I. Reduction and Oxidation. *Can. J. Chem.* **1972**, *50*, 3058-3062.
4. Scarborough, C. C.; Sproules, S.; Doonan, C. J.; Hagen, K. S.; Weyhermüller, T.; Wieghardt, K., Scrutinizing Low-Spin Cr(II) Complexes. *Inorg. Chem.* **2012**, *51*, 6969-6982.
5. Hagen, W. R., Wide zero field interaction distributions in the high-spin EPR of metalloproteins. *Mol. Phys.* **2007**, *105*, 2031-2039.
6. Stoll, S.; Schweiger, A., EasySpin, a comprehensive software package for spectral simulation and analysis in EPR. *J. Magn. Reson.* **2006**, *178*, 42-55.
7. Sheldrick, G., A short history of SHELX. *Acta Crystallographica Section A* **2008**, *64*, 112-122.
8. Bruker APEX2, Bruker AXS Inc.: Madison, Wisconsin, USA, 2012.
9. Weigend, F.; Ahlrichs, R., Balanced basis sets of split valence, triple zeta valence and quadruple zeta valence quality for H to Rn: Design and assessment of accuracy. *Physical Chemistry Chemical Physics* **2005**, *7*, 3297-3305.
10. Schäfer, A.; Huber, C.; Ahlrichs, R., Fully optimized contracted Gaussian basis sets of triple zeta valence quality for atoms Li to Kr. *J. Chem. Phys.* **1994**, *100*, 5829-5835.
11. Schäfer, A.; Horn, H.; Ahlrichs, R., Fully optimized contracted Gaussian basis sets for atoms Li to Kr. *J. Chem. Phys.* **1992**, *97*, 2571-2577.
12. Vosko, S. H.; Wilk, L.; Nusair, M., Accurate spin-dependent electron liquid correlation energies for local spin density calculations: a critical analysis. *Can. J. Phys.* **1980**, *58*, 1200-1211.
13. Lee, C.; Yang, W.; Parr, R. G., Development of the Colle-Salvetti correlation-energy formula into a functional of the electron density. *Physical Review B* **1988**, *37*, 785-789.
14. Becke, A. D., Density-functional thermochemistry. III. The role of exact exchange. *J. Chem. Phys.* **1993**, *98*, 5648-5652.
15. Frisch, M. J.; Trucks, G. W.; Schlegel, H. B.; Scuseria, G. E.; Robb, M. A.; Cheeseman, J. R.; Scalmani, G.; Barone, V.; Petersson, G. A.; Nakatsuji, H.; Li, X.; Caricato, M.; Marenich, A.

V.; Bloino, J.; Janesko, B. G.; Gomperts, R.; Mennucci, B.; Hratchian, H. P.; Ortiz, J. V.; Izmaylov, A. F.; Sonnenberg, J. L.; Williams; Ding, F.; Lipparini, F.; Egidi, F.; Goings, J.; Peng, B.; Petrone, A.; Henderson, T.; Ranasinghe, D.; Zakrzewski, V. G.; Gao, J.; Rega, N.; Zheng, G.; Liang, W.; Hada, M.; Ehara, M.; Toyota, K.; Fukuda, R.; Hasegawa, J.; Ishida, M.; Nakajima, T.; Honda, Y.; Kitao, O.; Nakai, H.; Vreven, T.; Throssell, K.; Montgomery Jr., J. A.; Peralta, J. E.; Ogliaro, F.; Bearpark, M. J.; Heyd, J. J.; Brothers, E. N.; Kudin, K. N.; Staroverov, V. N.; Keith, T. A.; Kobayashi, R.; Normand, J.; Raghavachari, K.; Rendell, A. P.; Burant, J. C.; Iyengar, S. S.; Tomasi, J.; Cossi, M.; Millam, J. M.; Klene, M.; Adamo, C.; Cammi, R.; Ochterski, J. W.; Martin, R. L.; Morokuma, K.; Farkas, O.; Foresman, J. B.; Fox, D. J. *Gaussian 16 Rev. C.01*, Wallingford, CT, 2016.